CONTRAST SENSITIVITY TO ONE- AND TWO-DIMENSIONAL LUMINANCE PATTERNS

Steven S. Persaud

Thesis submitted to the faculty of the Virginia Polytechnic Institute and State University
in partial fulfillment of the requirements for the degree of

Master of Science
In
Industrial and Systems Engineering

Dr. Robert J. Beaton, Chair
Dr. Brian M. Kleiner
Dr. Albert M. Prestrude

May 5, 2004
Blacksburg, Virginia
Keywords: contrast sensitivity, luminance, spatial vision, Fourier analysis

CONTRAST SENSITIVITY TO ONE- AND TWO-DIMENSIONAL LUMINANCE PATTERNS

Steven S. Persaud

(ABSTRACT)

Contrast sensitivities to one- and two-dimensional luminance patterns were compared in a two-alternative forced choice (2AFC) experiment. Space-averaged luminance was also manipulated. Statistical analyses revealed a main effect of stimulus dimension ($p < .05$) and no effect of space-averaged luminance. The main effect of stimulus dimension was explained in terms of an on-center, off-center receptive field model combined with watershed spatial vision behavior at spatial frequencies below 1 cycle-per-degree (cpd). The non-significant result for space-averaged luminance was explained by the limited range of manipulation of the variable. Two-dimensional luminance patterns were suggested as ideal patterns for reconciling grating-based spatial vision research with spatial vision behavior in an ecological context. Future research directions are suggested.

DEDICATION

To Mom and Dad for their encouragement and support throughout this endeavor.

ACKNOWLEDGEMENT

I would like to gratefully acknowledge my advisor, Dr. Robert J. Beaton. Without his guidance, advice, and support this work would not have been possible.

I would also like to thank my committee members, Dr. Albert M. Prestrude and Dr. Brian M. Kleiner, for their support and patience in seeing this project through to its end.

To Lovedia Cole and the Industrial and Systems Engineering staff, I express my gratitude for keeping me grounded in the formalities of an academic institution.

Lastly, I acknowledge those students, graduate and undergraduate, who endured my data collection procedure with enthusiasm.

LIST OF TABLES, FIGURES, AND EQUATIONS

Tables

Figures

Equations

TABLE OF CONTENTS

INTRODUCTION

Problem Presentation

The retinal image of a visual scene is two-dimensional in spatial extent. Yet, over the past 40 years, vision scientists have investigated early spatial vision predominantly in terms of contrast sensitivity to one-dimensional luminance patterns, such as sinusoidal gratings. Researchers have justified this approach through Fourier analysis, a reversible mathematical process that enables researchers to describe a two-dimensional visual scene in terms of individual sinusoidal components of varying phase, orientation, magnitude, and frequency. These characteristics are fully encompassed by a sinusoidal grating, and thus a grating provides a simple tool for investigating early spatial vision (Regan, 2000; Wandell, 1995).

Grating research has led scientists to model early spatial vision as an array of linear filters, each tuned to a narrow range of spatial frequencies and orientations (Graham, 1989; Olzak & Thomas, 1986; Regan, 2000; Wandell, 1995). This array is thought to operate in parallel, with each filter simultaneously analyzing small patches (or receptive fields) of the retinal image for subsequent processing in the visual cortex (Campbell & Robson, 1968; Robson, 1975). The linear and parallel nature of this spatial vision model enables a single filter to be representative of any other filter that is sensitive to the same range of spatial frequencies but at different orientations (Caelli, Brettel, Rentschler, and Hilz, 1983). Consequently, one-dimensional spatial vision, characterized by one-dimensional stimuli, should be representative of two-dimensional spatial vision, characterized by two-dimensional stimuli.

A small but growing body of literature has revealed that two-dimensional spatial vision is not adequately described by data obtained from one-dimensional spatial vision experiments (e.g., Derrington & Henning, 1989; Kelly & Magnuski, 1975; Olacsi, 2001; Wilkinson, Wilson, & Habak, 1998). Visual response to two-dimensional stimuli has been associated with higher detection thresholds (Kelly & Magnuski, 1975); broader and stronger masking effects (Derrington & Henning, 1989; Olacsi, 2001); and better vernier acuity (Wilkinson et al., 1998). Clearly, a spatial vision model solely based upon grating data cannot fully describe two-dimensional spatial vision. Data describing two-dimensional spatial vision, in terms of response to two-dimensional stimuli, are exceedingly scarce – more data are required.

Research Aims

The motivation for this research is to contribute additional knowledge to the growing body of literature focusing on two-dimensional spatial vision. Specifically, this research extends the work of Olacsi (2001). Olacsi (2001) conducted a series of experiments that demonstrated the advantages of utilizing two-dimensional spatial vision in a real-world, engineering application. In his first experiment, he found evidence indicating that two-dimensional masking extended over a greater spatial bandwidth than one-dimensional masking and also exhibited an asymmetric, upward spread of masking. In other experiments, Olacsi (2001) applied these findings to target detection and recognition tasks involving military vehicles in natural camouflage. He found that threshold elevation data, obtained from two-dimensional masking, could be used to predict masked thresholds in real-world scenes.

Olacsi (2001) was unable to offer a complete explanation for this practical application of two-dimensional spatial vision because the relationship between sensitivity to one- and two-dimensional visual stimuli had not been investigated and existing literature did not provide sufficient guidance – two-dimensional spatial vision has not been systematically investigated since the pioneering work of Kelly and Magnuski (1975), 30 years earlier. The motivation for this research is to fill the gap left in Olasci (2001) through an investigation of two-dimensional spatial vision in a threshold experiment similar to the work of Kelly and Magnuski (1975). Threshold experiments typically provide clearer insight into eye-brain mechanisms (Wandell, 1995), and a direct comparison of one- vs. two-dimensional stimuli is an important contribution to the development of theoretical perspectives on two-dimensional spatial vision.

In addition to comparing stimulus dimensions, space-averaged luminance was manipulated to explore the effect of the eye's optics on two-dimensional spatial vision. Space-averaged luminance has well documented properties in relation to one-dimensional spatial vision (Norton, Lakshminarayanan, & Bassi, 2002; Olzak & Thomas, 1986; Thomas, 1975) and including it as an independent variable might provide additional insight into two-dimensional spatial vision. The specific aims of this research were to evaluate the following hypotheses in order to explore the relationship between one- and two-dimensional spatial vision:

- Stimulus Dimension: H_0: $\mu_{1D} - \mu_{2D} = 0$, H_1: $\mu_{1D} - \mu_{2D} \neq 0$. This hypothesis evaluates the effect of stimulus dimension, one-dimensional (μ_{1D}) vs. two-dimensional (μ_{2D}) luminance patterns.

- Space-averaged Luminance: H_0: $\mu_{high} - \mu_{low} = 0$, H_1: $\mu_{high} - \mu_{low} \neq 0$. This hypothesis evaluates the effect of space-averaged luminance, high (μ_{high}) vs. low (μ_{low}) space-averaged luminance.

REVIEW OF LITERATURE

One-Dimensional Spatial Vision

Theoretical and Practical Perspectives

Spatial vision – the way we view our world through visual discrimination of spatially defined features – has been investigated through research involving sinusoidal grating patterns (Regan, 2000; Wandell, 1995). From a theoretical perspective, contemporary theory describes spatial vision as an array of linear filters, each tuned to a narrow range of spatial frequencies and orientation (Graham, 1989; Olzak & Thomas, 1986; Regan, 2000; Wandell, 1995). Therefore, sinusoidal grating patterns, which represent pure spatial frequency at a specific orientation, provided researchers with a excellent instrument for investigation of theoretical spatial vision filters (Wandell, 1995).

From a practical perspective, generating sinusoidal grating patterns do not require sophisticated equipment and thus provided an easily accessible tool for investigating spatial vision (Kelly & Magnuski, 1975). In addition, analysis of sinusoidal gratings required fewer computational resources compared to analysis of a full, two-dimensional visual scene (Olacsi, 2001). With the advent of modern computing, these representational and computational challenges are no longer present (Olacsi, 2001). Consequently, a small but growing body of literature has begun to challenge contemporary spatial vision models that were developed from grating research.

Filter Model of Spatial Vision

Campbell and Robson (1968) conducted an investigation of contrast sensitivity to sinusoidal, square-wave, and saw-tooth gratings. They found that contrast sensitivity was a function of each waveform's component of maximum amplitude in Fourier space. Moreover, Campbell and Robson found that observers could not distinguish a square waveform from an equivalent sinusoid until the square waveform's 3rd harmonic reached its own independent threshold. Thus, early spatial vision could be approximated by a modest Fourier analyzer (Robson, 1975) and described by selective rather than broadband filter mechanisms (Thomas, 1975). Vision researchers have widely accepted this notion of frequency selective, linear filter mechanisms.

Caelli et al. (1983) extended the notion of selective filters to include orientation selectivity. They conducted a visual discrimination experiment to determine regions of non-discrimination for bands for filters (i.e., filters sensitive to the same range of spatial frequencies but at different orientations). Caelli et al. (1983) utilized paired sinusoidal

gratings that varied in both spatial frequency and orientation, thus eliciting a rudimentary two-dimensional visual response. They found that spatial frequency discriminability was independent of orientation. In other words, spatial frequency discriminability at a selected orientation predicted discriminability of the same spatial frequency at all other orientations. Caelli et al. (1983) found that orientational selectivity bandwidth ranged from 1° to 5°, depending upon spatial frequency. Thus, frequency selective, linear filter spatial vision mechanisms could be extended to include orientational selectivity.

Role of Fourier Analysis

The ability to characterize spatial vision in terms of response to sinusoids enables vision scientists to describe a two-dimensional luminance pattern in terms of its one-dimensional components. Thus, the retinal image, which is two-dimensional in spatial extent, can be represented by the contribution of individual spatial vision filter mechanisms. Indeed, Fourier analysis of spatial frequency has been accepted as the preferred method for characterizing imaging systems, including the human vision system (Bracewell, 1986; Graham, 1989; Norton et al., 2002; Watanabe, Mori, Nagata, & Hiwatashi, 1968).

Fourier analysis transforms complex waveforms, such as those present in a two-dimensional visual scene, into pure sinusoidal waveforms of varying phase, orientation, magnitude, and frequency. For spatial vision, this transformation is constrained to the luminance content of the original scene. Sinusoidal waveforms obtained through Fourier analysis can be realized by individual sinusoidal gratings, as demonstrated by Campbell and Robson (1968).

Transition to Two-dimensions

Grating research had proven invaluable in investigating and modeling early spatial vision. Indeed, models developed from grating research have proven useful in computer graphics and other applied, engineering settings (Beaton, 1983; Ferwerda, Shirley, Pattanaik, & Greenberg, 1997). Unfortunately, a small but growing body of literature has revealed that a spatial vision model based solely upon grating data cannot fully describe two-dimensional spatial vision (e.g., Derrington & Henning, 1989; Kelly & Magnuski, 1975; Wilkinson et al., 1998).

Two-dimensional Spatial Vision

Limitations of Grating Research

Derrington and Henning (1989) investigated filter selectivity in a simple visual masking experiment that utilized mixed sinusoidal gratings in a stimulus paradigm similar to the one employed by Caelli et al. (1983). Derrington and Henning (1989) utilized a vertically-oriented sinusoidal grating, modulated at 3 cycles per degree (cpd), as the target grating. They measured threshold elevation under three experimental conditions: (a) target grating alone; (b) target grating mixed with a single, 3 cpd mask grating oriented at +45 degrees from vertical; and (c) target grating mixed with a pair of 3 cpd mask gratings respectively oriented at ±45 degrees from vertical. Derrington and Henning (1989) found that threshold elevation with the pair of mask gratings could not be predicted from data involving a single mask grating – threshold elevation with the pair of mask gratings was stronger than anticipated. Based upon their findings, Derrington and Henning (1989) acknowledged the challenge of describing two-dimensional spatial vision within the contemporary framework of selective filters tuned to narrow ranges of spatial frequency and orientation.

Two-dimensional Pattern Research

Kelly and Magnuski (1975) provided a more direct challenge to contemporary spatial vision models in a contrast sensitivity experiment that examined sensitivity to one- and two-dimensional luminance patterns. Contemporary spatial vision theory holds that contrast sensitivity to a one-dimensional luminance pattern should predict sensitivity to a two-dimensional luminance pattern of equivalent spatial frequency. Kelly and Magnuski (1975) found that this was not the case – sensitivity to two-dimensional luminance patterns was lower than sensitivity to one-dimensional luminance patterns at spatial frequencies greater than 1 cpd. Both luminance patterns produced contrast sensitivity roll-off at low spatial frequencies (< 1 cpd), consistent with the watershed model suggested by Campbell, Johnstone, and Ross (1981).

In their data analysis, Kelly and Magnuski (1975) found that one-dimensional Fourier transforms, appropriate to one-dimensional stimuli and linear systems analysis, could not describe their findings. Two-dimensional Fourier transforms, on the other hand, enabled Kelly and Magnuski (1975) to describe their data in terms of a peak-detector visual mechanism operating in the Fourier domain. Specifically, they found that detection thresholds, in two-dimensional spatial vision, appeared to be mediated by a detector mechanism sensitive to peak components in the two-dimensional Fourier transform.

Peak-detector behavior of the spatial vision system at threshold is not strictly confined to two-dimensional visual stimuli. Campbell and Robson (1968) noted similar findings in their research with square and triangle waveform gratings. Similarly, Greenlee and Magnussen (1987) found that the spatial vision responded to peak components in their research with square waveform gratings. Greenlee and Magnussen (1987) also found evidence that the spatial vision system operated as a harmonic analyzer, exhibiting adaptation to the fundamental frequency of a missing-fundamental, square-waveform grating.

Wilkinson et al. (1998) provided limited but relevant support to the research findings of Kelly and Magnuski (1975). Wilkinson et al. (1998) examined visual discrimination thresholds for perturbations in four cycles of one- and two-dimensional D4 patches (fourth spatial derivative of a Gaussian patches). They found that discrimination thresholds were lower for perturbations of two-dimensional D4 patches compared to one-dimensional D4 patches. Wilkinson et al. (1998) did not further investigate this finding but concluded that visual processes underlying one- and two-dimensional spatial vision were not the same.

Olacsi (2001) conducted a series of experiments that demonstrated the advantages of utilizing two-dimensional spatial vision in a real-world, engineering application. In his first experiment, Olacsi (2001) investigated the properties of two-dimensional masking using radial luminance patterns (concentric circles) as stimuli. He found evidence indicating that two-dimensional masking extended over a greater spatial bandwidth than one-dimensional masking. Two-dimensional masking also exhibited an asymmetric, upward spread of masking.

In other experiments, Olacsi (2001) applied these findings to target detection and recognition tasks involving military vehicles in natural camouflage. He found that threshold elevation data, obtained from two-dimensional masking, could be used to predict masked thresholds in real-world scenes. Olacsi (2001) was unable to offer a complete explanation for this practical application of two-dimensional spatial vision because the relationship between sensitivity to one- and two-dimensional visual stimuli had not been investigated and existing literature did not provide sufficient guidance.

The motivation for this research was to investigate the relationship between one- and two-dimensional spatial vision and extend the work of Olacsi (2001).

Summary

Over the past 40 years, grating research has enabled vision scientists to construct a robust model of the spatial vision system (Graham, 1989; Olzak & Thomas, 1986; Regan, 2000; Wandell, 1995). This model has enjoyed a great deal of popularity and has practical applications in applied settings, such as computer graphics (Beaton, 1983; Ferwerda, Shirley, Pattanaik, & Greenberg, 1997). In general, this model depicts spatial vision processing as follows:

- An array of linear filters, each tuned to a narrow range of spatial frequencies and orientations (Campbell & Robson, 1968; Caelli et al., 1983);
- Array is thought to operate in parallel, each filter simultaneously analyzing small patches of the retinal image for subsequent processing in the visual cortex (Robson, 1975);
- A linear system capable of fully describing visual response to two-dimensional image in terms of its one-dimensional Fourier components (Bracewell, 1986; Watanabe, Mori, Nagata, & Hiwatashi, 1968).

A small but growing body of literature has revealed that a spatial vision model solely based upon grating data cannot fully describe two-dimensional spatial vision (e.g., Derrington & Henning, 1989; Kelly & Magnuski, 1975; Wilkinson et al., 1998). In general, visual response to two-dimensional stimuli has been associated with:

- Less sensitive (higher) detection thresholds (Kelly & Magnuski, 1975);
- Broader and stronger masking effects (Derrington & Henning, 1989; Olacsi, 2001);
- Better vernier acuity (Wilkinson et al., 1998).

Research describing spatial vision in terms of response to two-dimensional stimuli is scarce. Consequently, experimental data for modeling two-dimensional spatial vision are in short supply. Additional research with two-dimensional stimuli is required to develop a better theoretical understanding of two-dimensional spatial vision. The motivation for this research was extend the work of Olacsi (2001) and contribute additional knowledge to the research domain focusing on two-dimensional spatial vision.

METHODS

Experiment Setup

Participants

Ten individuals (3 female) were recruited from the student population at Virginia Tech. Each individual demonstrated normal spatial vision on the VisTech VCTS 6500 test system (VisTech, 1990) before participating in the experiment. Participants were compensated $21 for the 3-hour experimental session ($7/hour).

Apparatus

A Dell Precision 620 workstation provided a highly-automated experimental control and data collection system. The only experimenter inputs were participant and trial information. The computer handled experimental scripting, stimulus presentation, and data recording. The following hardware and software were installed in the computer system:

- High-quality Matrox Millennium G450 video graphics accelerator;
- Microsoft Windows 2000 SP4 operating system;
- Neurometrics Institute (2003) WinVis W4M stimulus generation and experimental scripting software system; and
- Mathworks Matlab version 6.5R13 programming language.

Visual stimuli were presented on a Tektronix GMA 201 high-resolution monochrome CRT monitor (19" (48 cm) diagonal). High bandwidth BNC connectors were used to connect the CRT monitor to the video graphics accelerator. A Minolta CS100 spot photometer mounted on a tripod was used to perform photometric measurements.

Experimental Design

A $2 \times 2 \times 4$ within-subject, full-factorial experimental design was employed in this experiment (shown as Figure 1).

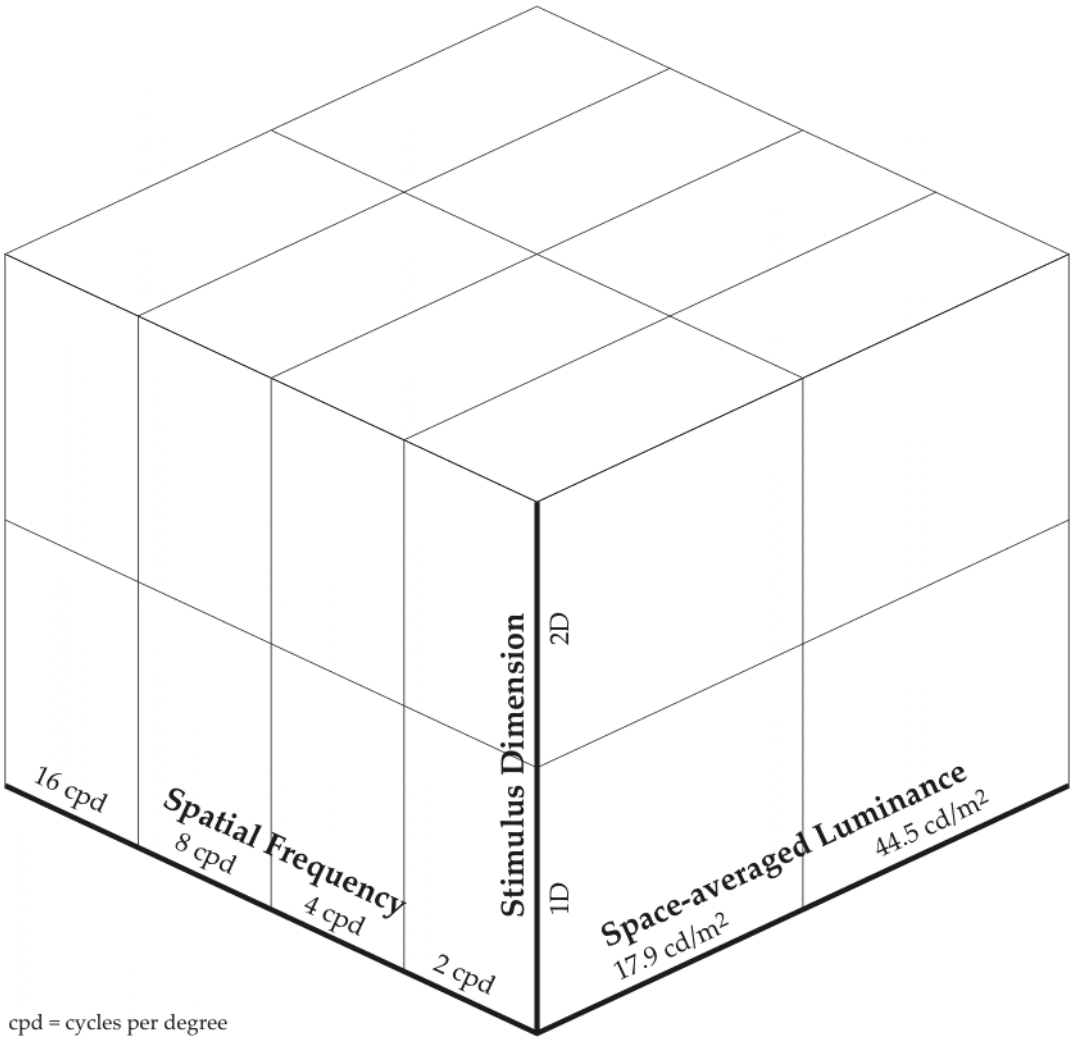

Figure 1. Experimental design matrix

Viewing Conditions

Viewing Geometry

Figure 2 illustrates the viewing geometry for this research. The 15.8 cm × 15.8 cm target area subtended horizontal and vertical viewing angles of 5.75° × 5.75° at a viewing distance of 1.57 m. Horizontal and vertical viewing angles were selected to display a minimum of six cycles at the lowest tested spatial frequency of 2 cycles per degree (cpd). This restriction was necessary to avoid threshold elevation at low spatial frequencies due to limited number of cycles (see Hoekstra, Van Der Goot, Van Den Brink, & Bilsen, 1974). The observer was seated in a chair with a chin-rest positioned at the viewing distance.

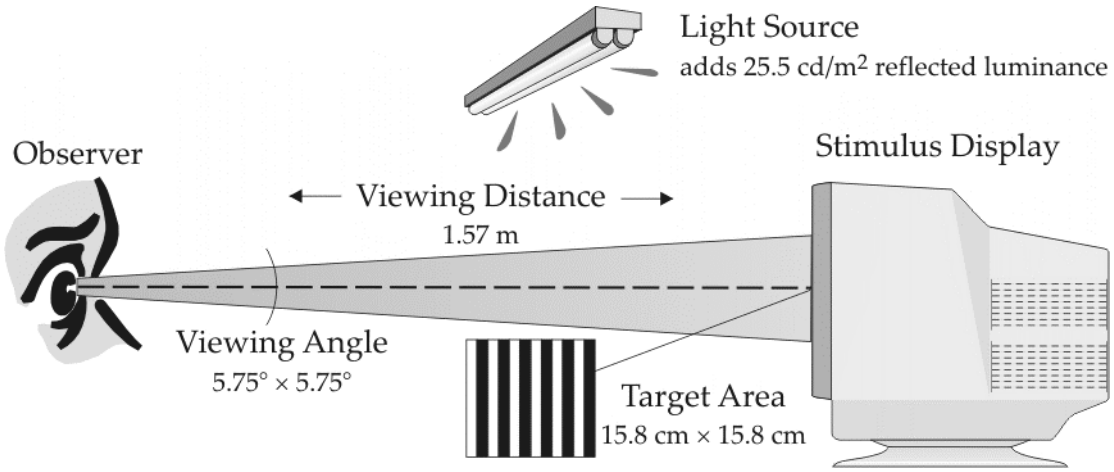

Figure 2. Viewing angle as a function of target area and viewing distance

Space-averaged Luminance

An overhead light source was used to manipulate space-averaged luminance, as illustrated in Figure 2. For low space-averaged luminance, the light source was switched off, and for high space-averaged luminance, the light source was switched on. When switched on, the light source added 25.5 cd/m^2 of diffusely reflected luminance (no glare) to the stimulus, increasing space-average luminance. Equation 1 shows the calculation of space-averaged luminance for one- and two-dimensional visual stimuli used in this research.

$$L_{avg} = \frac{L_{max} + L_{min}}{2} + L_{ref}$$

Equation 1

Where,

- L_{avg} is calculated space-averaged luminance;
- L_{max} is maximum pattern luminance, measured with lights switched off;
- L_{min} is minimum pattern luminance, measured with lights switched off; and
- L_{ref} is reflected luminance (zero with lights switched off and 25.5 cd/m^2 with lights switched on).

Space-averaged luminance was either 18 cd/m^2 (lights switched off, low space-averaged luminance) or 43.5 cd/m^2 (lights switched on, high space-averaged luminance).

Luminance Modulation

Luminance modulation was produced by modulating space-averaged luminance (Equation 1) with a sinusoidal waveform, as shown in Figure 3. The sinusoidal waveform is representative of one- and two-dimensional patterns used in this research.

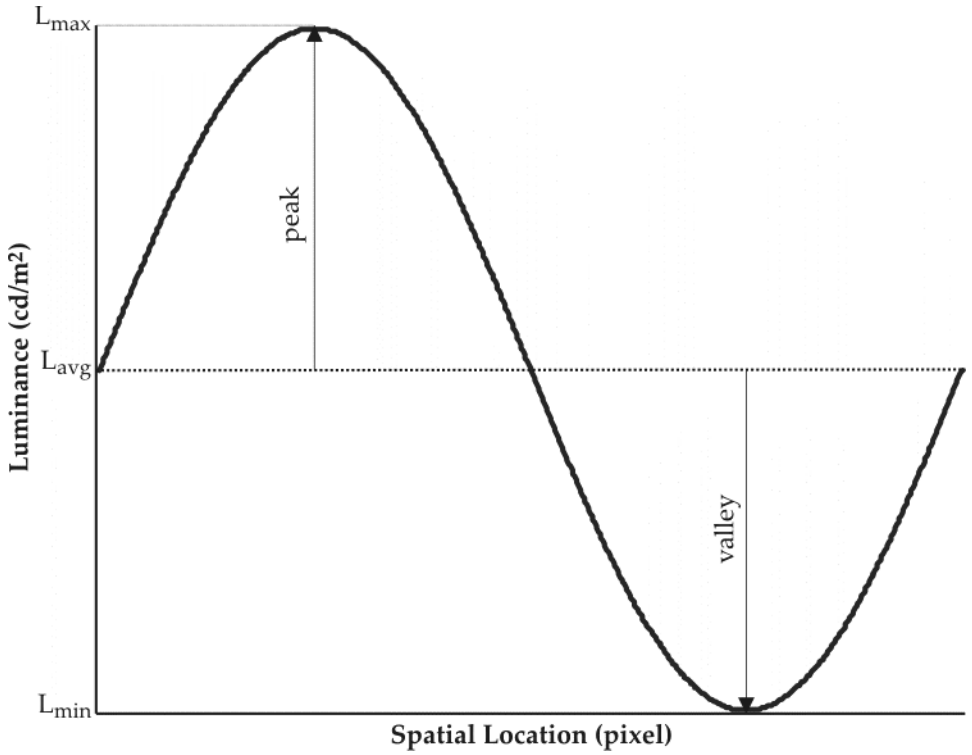

Figure 3. Sinusoidal modulation of space-averaged luminance

A formal mathematical definition of modulation is presented in Equation 2.

$$C = \frac{L_{max} - L_{min}}{L_{max} + L_{min} + 2L_{ref}} = \frac{L_{max} - L_{min}}{2} \times \frac{1}{L_{avg}}$$

Equation 2

Where,

- C is a unitless value representing modulation;
- L_{avg}, L_{max}, L_{min}, and L_{ref} are from Equation 1.

From Equation 2 and Figure 3, sinusoidal modulation can be understood as the ratio of amplitude (peak or valley) to space-averaged luminance. More generally, modulation is the ratio of one-half the peak-to-valley separation to space-averaged luminance.

Visual Stimuli

Visual stimuli consisted of one- and two-dimensional luminance patterns modulated at spatial frequencies of 2, 4, 8, and 16 cpd. Patterns were truncated by a Gaussian windowing function that constrained the viewing area to a 5 cpd viewing cone. Equation 3 and Equation 4 provide a formal mathematical definition of one- and two-dimensional luminance patterns.

$$L(m,n) = F(x,y,f) = C\sin(2\pi f x + \phi) \times e^{-4\ln 2\left(x^2 + y^2\right)/r^2}$$

Equation 3

$$L(m,n) = F(x,y,f) = C\sin(2\pi f \sqrt{x^2 + y^2} + \phi) \times e^{-4\ln 2\left(x^2 + y^2\right)/r^2}$$

Equation 4

Where (referring to Figure 4),

- L is luminance in cd/m^2;
- m and n are spatial coordinates in pixels;
- x and y are angular coordinates in degrees;
- C is a scalar value representing modulation;
- f is spatial frequency in cycles per degree;
- ϕ is initial phase in radians; and
- r is the radius of the Gaussian window in degrees.

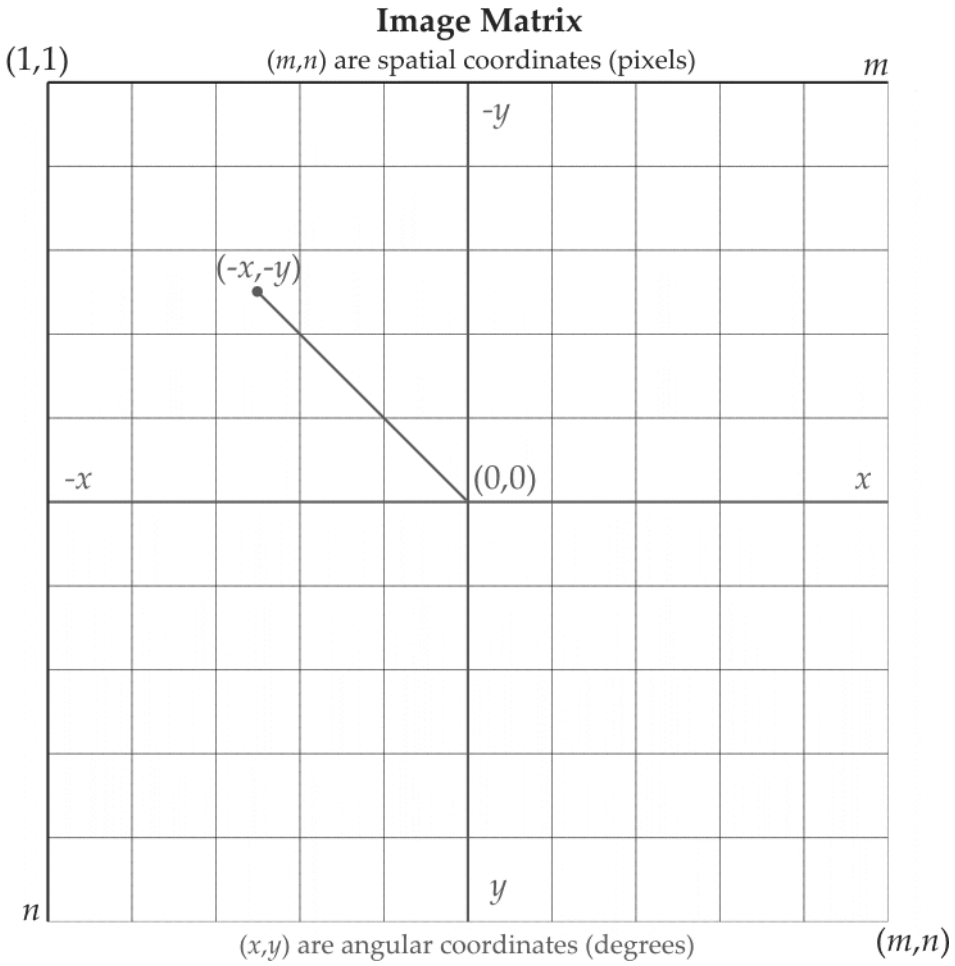

Figure 4. Image matrix

WinVis W4M software was used to generate visual stimuli as specified in Equation 3 and Equation 4. Examples of these stimuli are shown in Figure 5 and Figure 6.

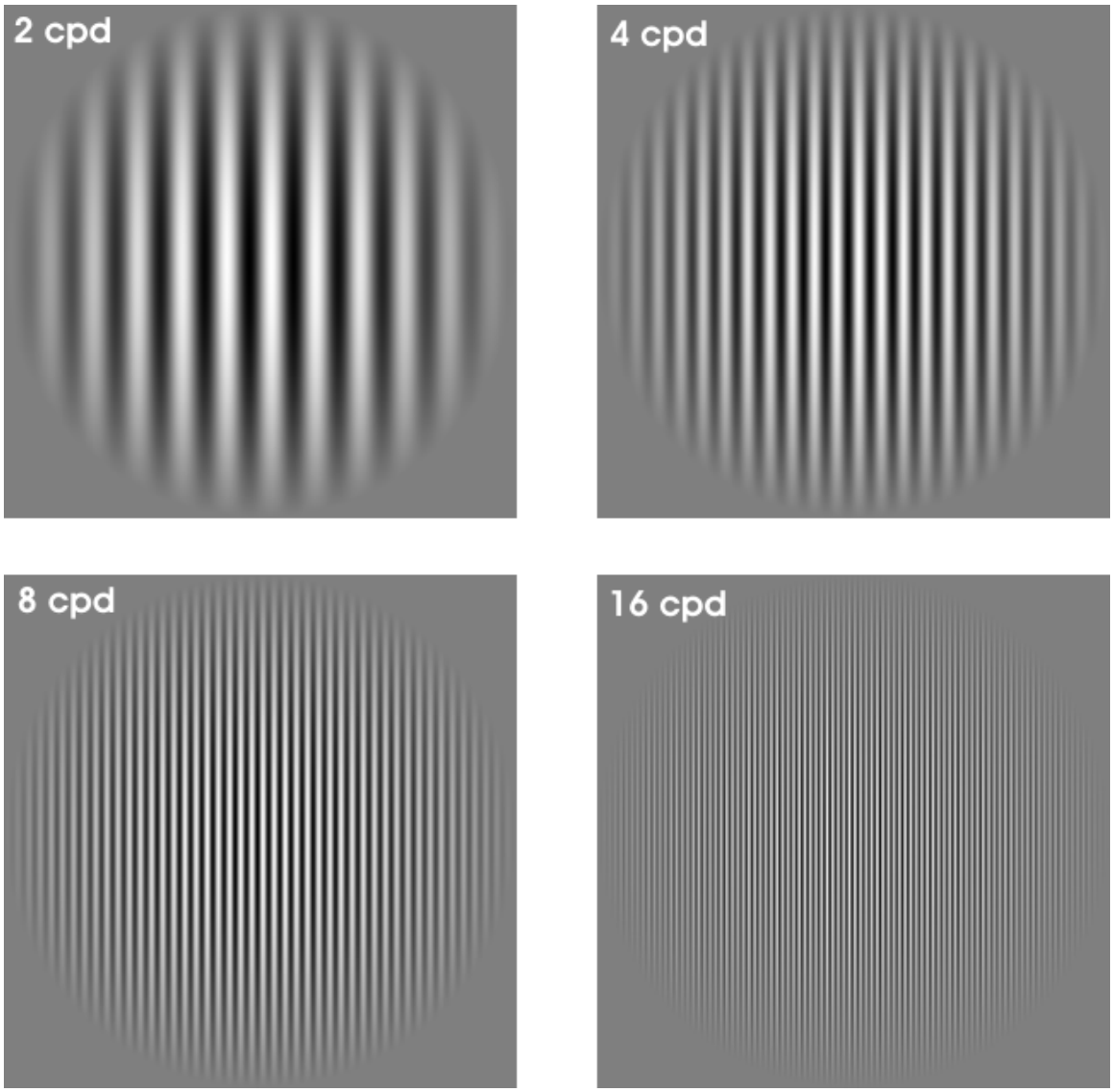

Figure 5. One-dimensional luminance patterns

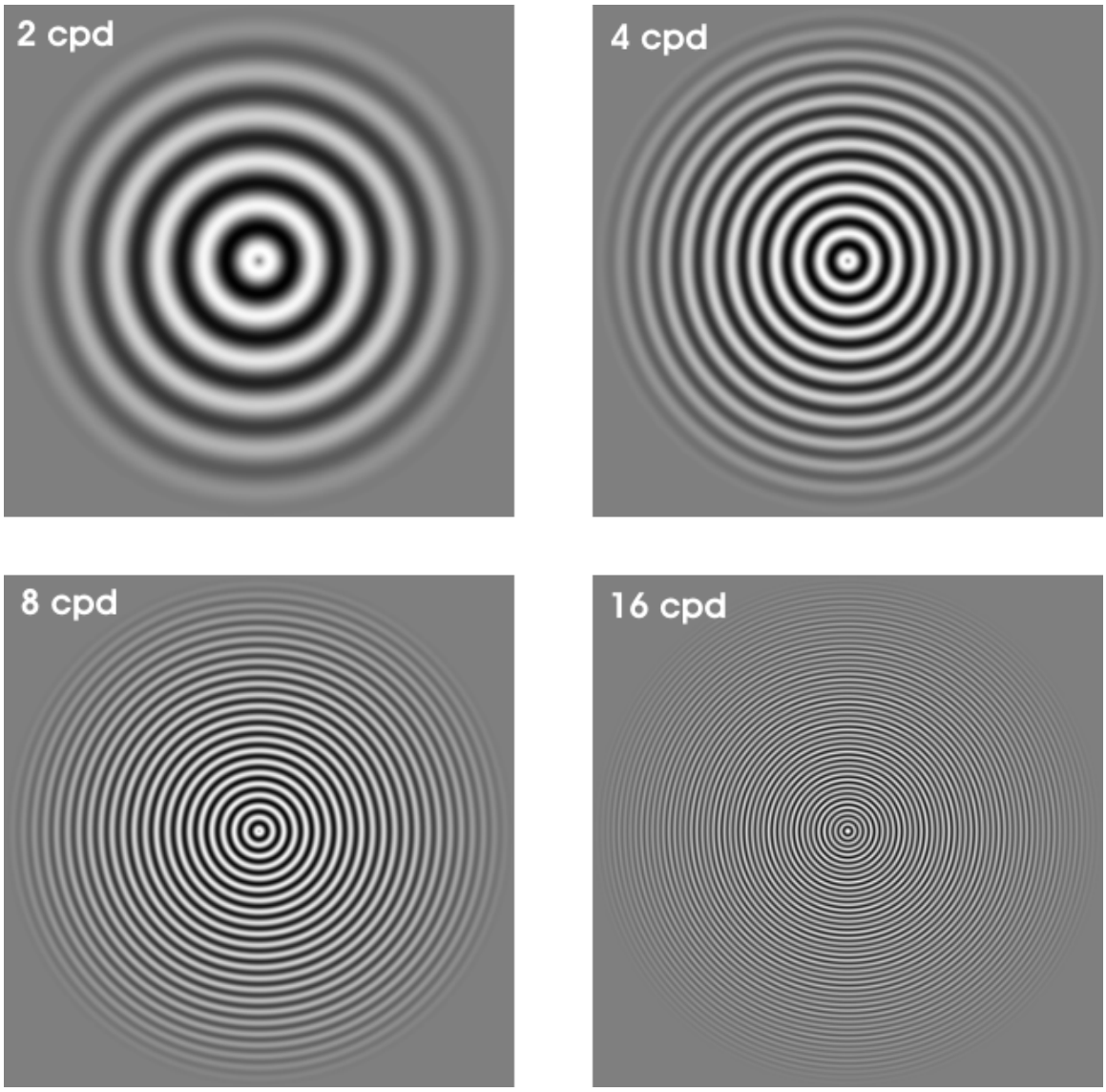

Figure 6. Two-dimensional luminance patterns

The software also provided a calibration utility for determining the gamma function (Equation 5) of the Tektronix GMA 201 CRT monitor and a linearization matrix (look-up table). The look-up table enabled values produced from F(x,y,f) to be mapped to a CRT luminance value.

$$L = A(v - v_0)^{\gamma} + L_0 = 4.92(v - 94.07)^{1.41} + 0.47$$

Equation 5

Where,

- L is on-screen luminance in cd/m^2, and

- v is input voltage supplied by WinVis W4M linearization routines.

WinVis W4M software did not include a reflected luminance (L_{ref}) term in the calculation of modulation (see Equation 2). As a result, modulation values supplied by WinVis W4M were equivalent to setting L_{ref} equal to zero (i.e., lights switched off). In order to include an L_{ref} term, modulation values were corrected by using Equation 6.

$$C_{lights-on} = \frac{C_{lights-off}}{1+\frac{L_{ref}}{L_{avg}}} = \frac{C_{lights-off}}{1+\frac{25.5\ cd/m^2}{18\ cd/m^2}}$$

Equation 6

Where,

$$(a)\ C_{lights-off} = \frac{L_{max}-L_{min}}{L_{max}+L_{min}}\ (from\ Equation\ 2)$$

$$(b)\ C_{lights-on} = \frac{L_{max}-L_{min}}{L_{max}+L_{min}+2L_{ref}}\ (from\ Equation\ 2)$$

$$(c)\ C_{lights-off} \times \frac{1}{1+\frac{2L_{ref}}{L_{max}+L_{min}}} = (b)$$

$$(d)\ from\ (c), \frac{1}{1+\frac{2L_{ref}}{L_{max}+L_{min}}} = \frac{1}{1+\frac{L_{ref}}{\frac{L_{max}+L_{min}}{2}}} = \frac{1}{1+\frac{L_{ref}}{L_{avg}}}\ (from\ Equation\ 1)$$

$$(e)\ thus, C_{lights-on} = C_{lights-off} \times \frac{1}{1+\frac{L_{ref}}{L_{avg}}} = \frac{C_{lights-off}}{1+\frac{25.5\ cd/m^2}{18\ cd/m^2}}\ (Equation\ 6)$$

Procedure

A two-alternative, forced-choice (2AFC) psychophysical method was used to collect data. This method is regarded as the most accurate and bias-free of the available psychophysical methods (Gescheider, 1997; Guildford, 1954; Macmillan & Creelman, 1991). In a 2AFC trial, an observer was presented with two stimulus intervals that were separated by a temporal interval. The observer was required to choose which of the two stimulus intervals contained an experimental stimulus. The level of the experimental stimulus was varied from trial-to-trial such that observer performance varied from 100% correct to chance-levels (50% correct).

WinVis W4M software included a 2AFC script that was used in this research. This script enabled the experimenter to specify the number of stimulus levels (5), trials per stimulus level (15), and inter-stimulus temporal interval (2s). The script randomized presentation of stimulus levels and administered the 2AFC procedure without further intervention from the experimenter. Observer performance data (proportion of correct responses) and trial information were automatically collected and stored in a Matlab binary file.

Presentation of spatial frequencies was randomized within blocks of stimulus dimension that were nested within blocks of space-averaged luminance (shown as Figure 7). Potential systematic bias arising from blocking was controlled by incompletely counterbalancing blocked variables such that each variable level preceded and followed every other variable level an equal number of times (Howell, 1987).

Participants observed a total of 16 different stimulus conditions (from Figure 1). Participants generally required 8 minutes to complete each stimulus condition, after which they were given a 2 minute rest period prior to continuing. Total experiment time was approximately 3 hours, including a 15 minute rest period halfway through the research session.

Space-averaged Luminance	Stimulus Dimension: 1D (1)	Stimulus Dimension: 2D (2)
Low (L)	L1 2, 4, 8, 16 cpd Randomized	L2 2, 4, 8, 16 cpd Randomized
High (H)	H1 2, 4, 8, 16 cpd Randomized	H2 2, 4, 8, 16 cpd Randomized

Block	Sequence
1	L1, L2, H1, H2
2	L1, L2, H2, H1
3	L2, L1, H1, H2
4	L2, L1, H2, H1
5	H1, H2, L1, L2
6	H1, H2, L2, L1
7	H2, H1, L1, L2
8	H2, H1, L2, L1

Figure 7. Blocking strategy

RESULTS

Introduction

The 2AFC procedure does not directly measure of observer thresholds. Rather, observer thresholds are empirically determined through a two-step procedure:

- The researcher chooses an observer performance level to represent threshold.
- The researcher fits a psychometric function to the 2AFC data set and uses this function to estimate threshold at the chosen observer performance level.

This procedure is not entirely bias free and may lead to overly optimistic and unreliable psychometric functions (Wichmann & Hill, 2001a). In order to minimize subjectivity in data analysis, an objective data analysis procedure was developed. This procedure was based upon recommendations from the literature. The following sections describe the development and application of this objective data analysis procedure.

Observer Performance Level

Klein (2001) defines threshold for m-AFC designs (e.g., 2AFC, 3AFC, 4AFC, etc.) as the proportion correct that corresponds to a d' value of 1, where d' is a measure of observer sensitivity within the framework of Signal Detection Theory (SDT). According to Klein (2001), the advantage of this definition is its independence from the m-AFC design used to collect data (i.e., it can be generalized across m-AFC designs).

For a 2AFC design, the threshold value for $d' = 1$ corresponds to an observer performance level of 76% correct response rate (Klein, 2001; Macmillan & Creelman, 1991). This reflects a 1% difference from the commonly used threshold definition of 75% correct response rate (Gescheider, 1997). In the interest of selecting a generalizable threshold definition, 76% correct response rate was chosen to represent observer performance at threshold.

Psychometric Functions

Software developed by Wichmann and Hill (2001a, 2001b) was used to fit Weibull functions to psychometric data generated by the 2AFC procedure. Weibull functions are used in visual psychophysics (Pelli as cited in Macmillan & Creelman, 1991) and provide excellent fits to psychometric data (Strasburger, 2001). The software used a

maximum likelihood estimation (MLE) procedure to fit Weibull functions to psychometric data (shown as Equation 7 from Wichmann & Hill, 2001a).

$$\psi(x) = \gamma + (1 - \gamma - \lambda)F(x, \alpha, \beta)$$

Equation 7

Where,

- ψ is observer performance in proportion of correct responses;
- x corresponds to stimulus value expressed as percent modulation;
- γ corresponds to the lower asymptote of ψ, which is equivalent to the guess rate (50% for 2AFC);
- λ corresponds to the upper asymptote of ψ, which is equivalent to the observer's lapse rate (0% for an ideal observer);
- F corresponds to a fitted Weibull function of the form $e^{-\left(\frac{x}{\alpha}\right)^{\beta}}$;
- α corresponds to the displacement of the Weibull function along the abscissa; and
- β corresponds to the slope of the Weibull function.

Equation 7 can be understood as equating observer performance, $\psi(x)$, to a fitted Weibull function, $F(x,\alpha,\beta)$, constrained by observer guess rate (γ) and lapse rate (λ). Constants, α and β, determine the scale and shape of the Weibull function. Guess rate (γ) is fixed at 50% because the observer has a 50% chance of choosing the correct interval in a 2AFC design. Lapse rate (λ) represents stimulus-independent lapses (blinking, fatigue, finger-error) when the stimulus is well above threshold and therefore, should always be detected (i.e., the difference between ideal and actual observer performance).

Data Presentation

Thresholds were determined using the procedure outlined in the preceding. In addition, psychometric functions were plotted and visually inspected to confirm threshold estimates. In several cases, plausible threshold estimates were not supported by visual inspection and were therefore excluded from further analysis. Statistical tests, such as Chi-square goodness-of-fit and bootstrap tests (Wichmann & Hill, 2001b), were attempted, but these tests proved to be insensitive in detecting poorly fitted psychometric functions.

Visual Inspection

Visual inspection was used to discriminate between acceptable and unacceptable psychometric fits. Although this procedure might appear to be subjective, it was based upon objective inspection criterion. Namely, The upper bound of a psychometric function should be adequately sampled by accurate observer performance in order to produce a reliable threshold estimate (Wichmann & Hill, 2001a). Therefore, psychometric fits that demonstrated minimum observer performance of 85% at the two highest stimulus levels were included in further data analysis. Psychometric fits that did not meet this visual inspection criterion were excluded from to further data analysis. Figure 8 and Figure 9 respectively illustrate accepted and rejected psychometric functions on the basis of the visual inspection criterion.

Examination of Figure 8 and Figure 9 reveals that Figure 8 exhibits an ogival shape that is characteristic of psychometric functions (Gescheider, 1997). The ogival shape of Figure 9 is less pronounced due to poor sampling at the higher stimulus levels – only a single point exceeds the defined threshold level. Wichmann and Hill (2001a) demonstrated that the ogival shape produced by Figure 9 leads to extreme variances in threshold estimation and unreliability in data analysis. Consequently, ogives that did not demonstrate at least 85% performance at the two highest stimulus levels were excluded from further data analysis. This criterion was applied without bias to the entire data set.

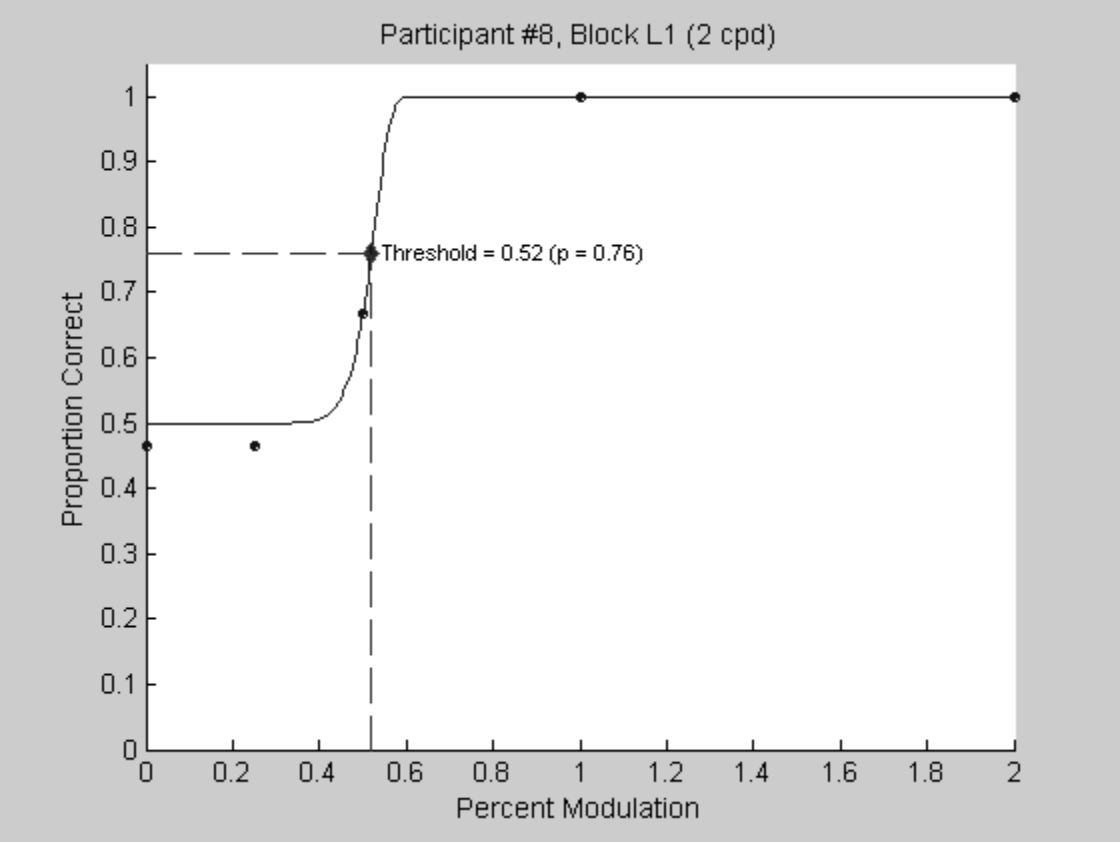

Figure 8. Accepted psychometric function

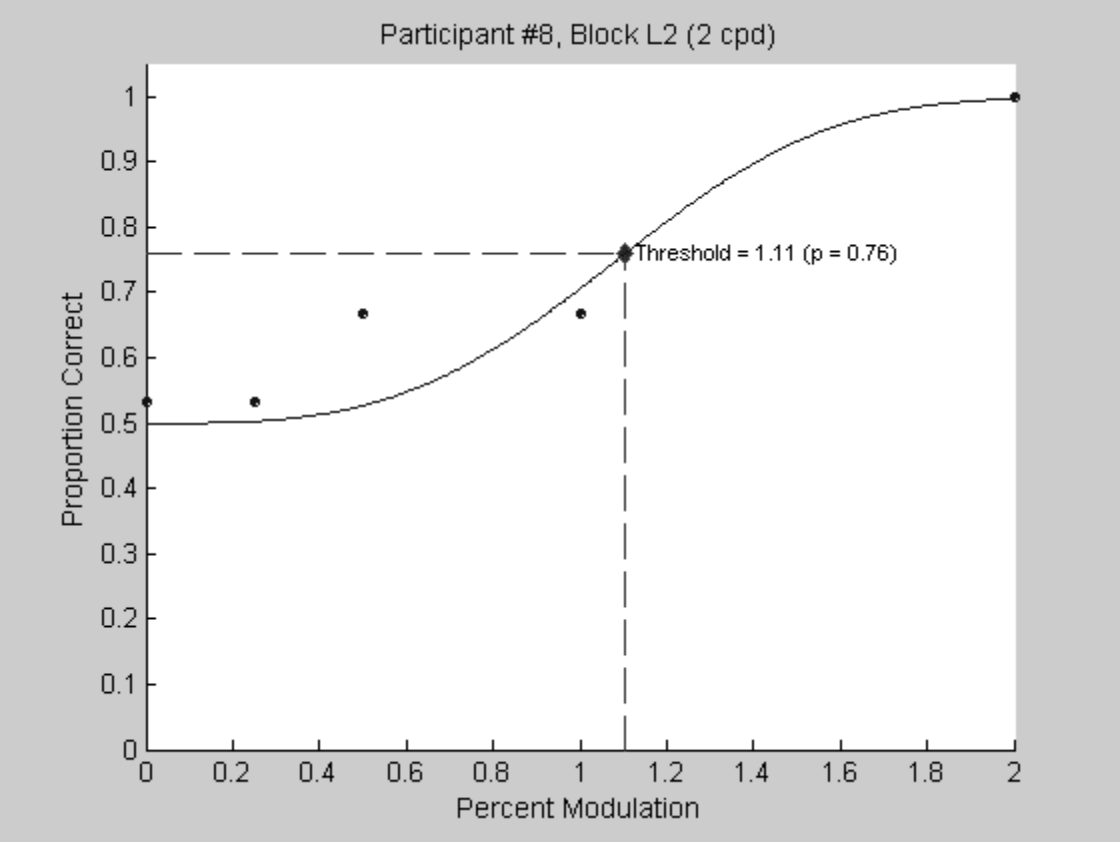

Figure 9. Rejected psychometric function

Data Tables

Table 1, Table 2, Table 3, and Table 4 summarize empirical threshold results for each tested spatial frequency. Threshold values are reported in terms of contrast sensitivity, which is the reciprocal of luminance modulation at threshold (i.e., 1 / threshold). Contrast sensitivity is a dimensionless quantity. Data for participants #4 and #8 were eliminated because both participants demonstrated a strong tendency for stimulus-independent lapses across all spatial frequencies. In other words, participants #4 and #8 demonstrated a tendency to respond independently of presence or absence of a stimulus.

Table 1
Contrast Sensitivity at 2 cpd

2 cpd	Contrast Sensitivity (1 / Threshold) × Block			
Participant #	**H1**[1]	**H2**[1]	**L1**[1]	**L2**[1]
2	476	excluded	268	169
3	168	excluded	137	76
5	236	excluded	168	148
6	317	206	169	268
7	excluded	excluded	169	142
9	excluded	197	169	171
10	excluded	excluded	147	78
11	412	412	171	272
Total N	5	3	8	8

[1]From Figure 7:
H1 = High space-averaged luminance × One-dimensional pattern
H2 = High space-averaged luminance × Two-dimensional pattern
L1 = Low space-averaged luminance × One-dimensional pattern
L2 = Low space-averaged luminance × Two-dimensional pattern

Table 2
Contrast Sensitivity at 4 cpd

4 cpd	Contrast Sensitivity (1 / Threshold) × Block			
Participant #	**H1**[1]	**H2**[1]	**L1**[1]	**L2**[1]
2	176	excluded	268	169
3	excluded	excluded	excluded	97
5	252	excluded	166	133
6	252	excluded	268	197
7	excluded	excluded	195	97
9	168	excluded	272	148
10	168	excluded	141	131
11	323	205	267	197
Total N	6	1	7	8

[1]From Figure 7:
H1 = High space-averaged luminance × One-dimensional pattern
H2 = High space-averaged luminance × Two-dimensional pattern
L1 = Low space-averaged luminance × One-dimensional pattern
L2 = Low space-averaged luminance × Two-dimensional pattern

Table 3
Contrast Sensitivity at 8 cpd

8 cpd	Contrast Sensitivity (1 / Threshold) × Block			
Participant #	**H1**[1]	**H2**[1]	**L1**[1]	**L2**[1]
2	196	109	168	80
3	187	66	86	66
5	159	62	331	80
6	161	77	146	69
7	101	excluded	106	69
9	196	160	210	146
10	100	60	57	72
11	236	159	136	109
Total N	8	7	8	8

[1]From Figure 7:
H1 = High space-averaged luminance × One-dimensional pattern
H2 = High space-averaged luminance × Two-dimensional pattern
L1 = Low space-averaged luminance × One-dimensional pattern
L2 = Low space-averaged luminance × Two-dimensional pattern

Table 4
Contrast Sensitivity at 16 cpd

16 cpd	Contrast Sensitivity (1 / Threshold) × Block			
Participant #	**H1**[1]	**H2**[1]	**L1**[1]	**L2**[1]
2	161	113	67	26
3	129	excluded	excluded	excluded
5	excluded	excluded	excluded	45
6	143	excluded	61	42
7	82	excluded	33	excluded
9	excluded	excluded	65	26
10	excluded	excluded	excluded	26
11	159	62	61	41
Total N	5	2	5	6

[1]From Figure 7:
H1 = High space-averaged luminance × One-dimensional pattern
H2 = High space-averaged luminance × Two-dimensional pattern
L1 = Low space-averaged luminance × One-dimensional pattern
L2 = Low space-averaged luminance × Two-dimensional pattern

Examination of Table 1, Table 2, Table 3, and Table 4 reveals several instances of rejected psychometric fits on the basis of visual inspection. In particular, high space-averaged luminance data (H1 and H2) were significantly impacted at spatial frequencies of 2, 4, and 16 cpd. Both of these treatment conditions were very demanding, and participants might have been unduly susceptible to stimulus-independent lapses. Anecdotal comments by participants suggested that they habituated to guessing during demanding trials. In light of the low rate of data retention, all data for the high space-averaged luminance condition (H1 and H2) at 2, 4, and 16 cpd were excluded from further analysis. Sufficient data were obtained at 8 cpd to permit statistical comparison of high vs. low space-averaged luminance.

Data Exploration

Visualization

Prior to conducting statistical analysis, retained data were graphed to visualize the data trends and to better interpret statistical results (shown as Figure 10 and Figure 11). Summary statistics – mean, standard deviation (SD), and standard error of the mean (SEM) – were calculated within individual blocks, as presented in Table 1, Table 2, Table 3, and Table 4. Therefore, cell size (N) for summary statistics varied from block to block.

Figure 10 depicts contrast sensitivity curves for one- and two-dimensional luminance patterns at low space-averaged luminance. Data for the high space-averaged luminance condition were excluded. Thus, contrast sensitivity values were determined by averaging columns L1 and L2 in Table 1, Table 2, Table 3, and Table 4. Standard deviation (SD) and standard error of the mean (SEM) were calculated from the same columns.

Figure 11 depicts space-averaged luminance by stimulus dimension at 8 cpd. Similarly to Figure 10, the contrast sensitivity values were determined by averaging columns H1, H2, L1, and L2 from Table 3. Standard deviation (SD) and standard error of the mean (SEM) were calculated from the same columns.

Examination of Figure 10 reveals that the contrast sensitivity curve for one-dimensional luminance patterns exhibited a modest bandpass shape, peaking at 4 cpd. The contrast sensitivity curve for two-dimensional luminance patterns did not exhibit a similar peak, which is consistent with the findings of Kelly and Magnuski (1975). From Kelly and Magnuski (1975), one might expect this curve to peak at approximately 1 cpd; however, this spatial frequency was not evaluated in this research. Figure 10 also reveals that contrast sensitivity to one-dimensional luminance patterns was higher than contrast sensitivity to two-dimensional luminance patterns.

Examination of Figure 11 reveals a consistent effect of stimulus dimension. Namely, contrast sensitivity to one-dimensional luminance patterns was higher than sensitivity to two-dimensional luminance patterns. Figure 11 also reveals no effect of space-averaged luminance and no interaction between space-averaged luminance and stimulus dimension.

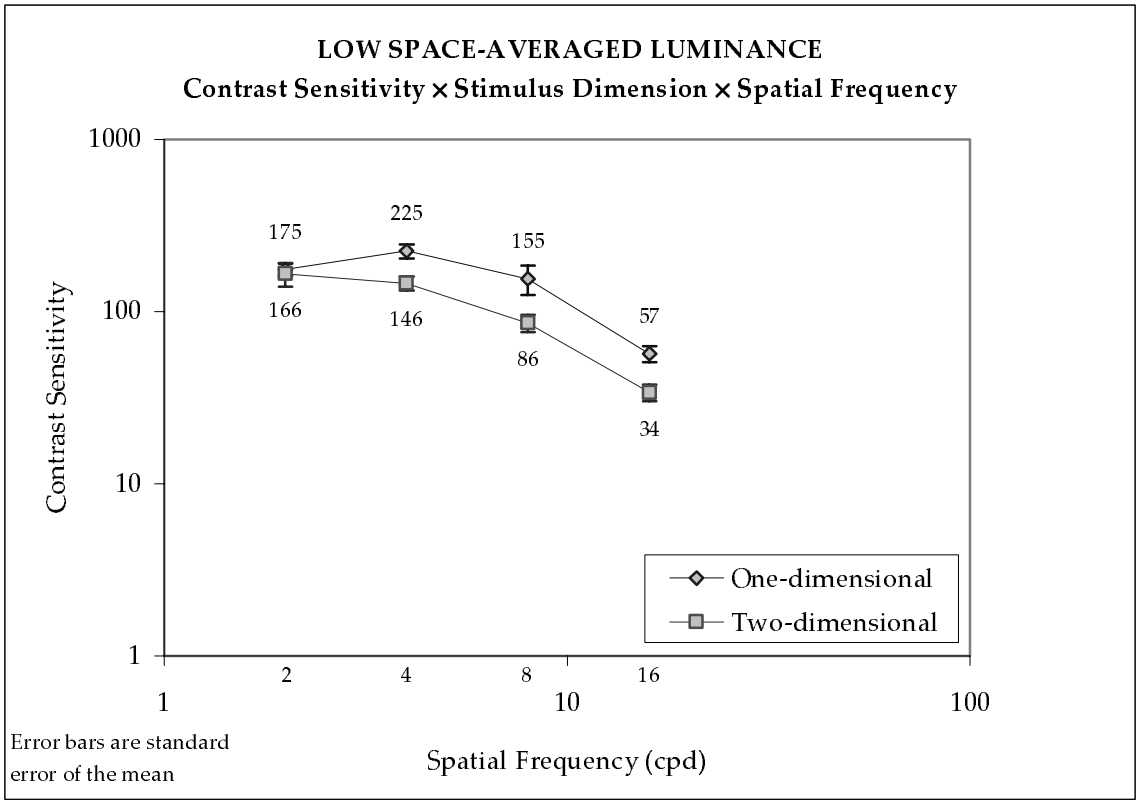

Figure 10. Contrast sensitivity × stimulus dimension × spatial frequency

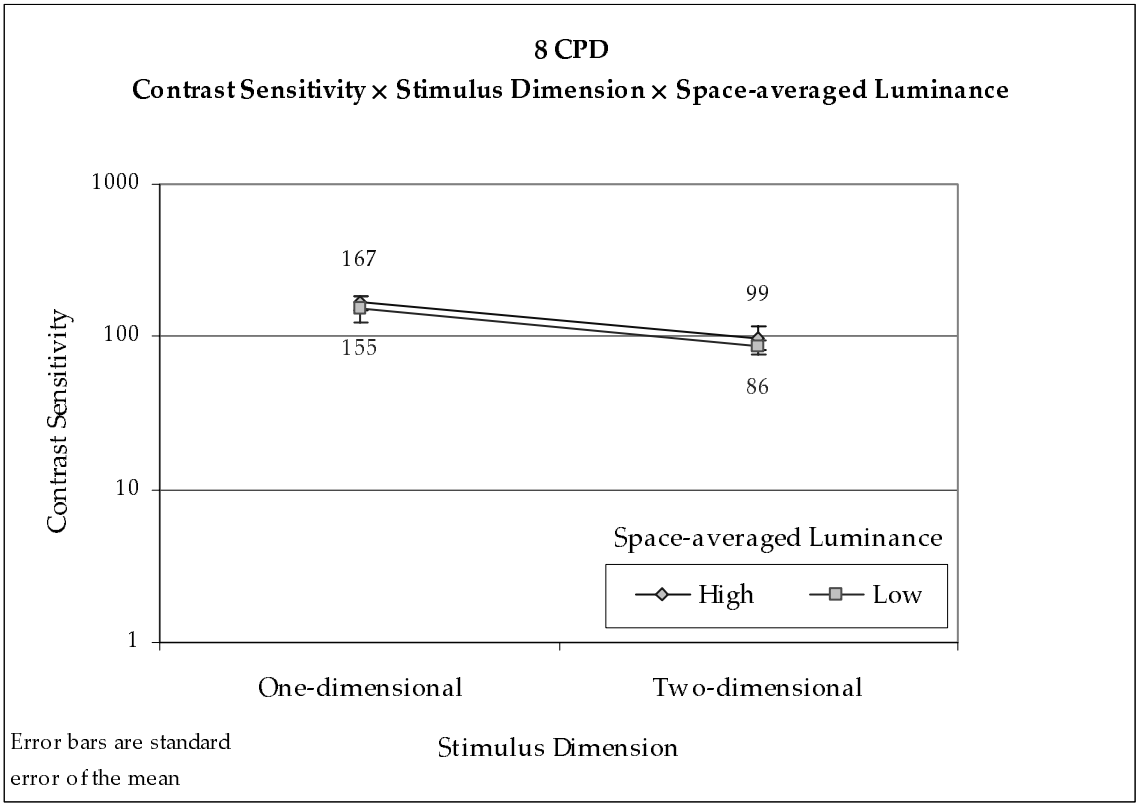

Figure 11. Contrast sensitivity × stimulus dimension × space-averaged luminance

Missing Data

Many statistical procedures, such as analysis of variance (ANOVA) or general linear model (GLM), cannot process unbalanced, within-subject data. Instead these procedures automatically eliminate cases with missing data in order to balance the design for further analysis. Due to this analysis restriction, 50% of retained data sets would have been omitted in a conventional statistical analysis. Consequently, missing data analysis was conducted in an effort to prevent data loss.

NORM software, developed by Schafer (1999), provided an expectation/maximization (EM) algorithm for imputing missing data values. Retained data sets were submitted to this algorithm which applied maximum likelihood estimation (MLE) to the data set in order to impute values of missing data. Results of this analysis are shown in Table 5.

Table 5
Imputed Data Values

Spatial Frequency	Participant #	Block	Imputed Value(s) (Contrast Sensitivity)	Original Table
4 cpd	3	L1	219	Table 2
8 cpd	7	H2	81	Table 3
16 cpd	3	L1, L2	44, 28	Table 4
"	5	L1	44	"
"	7	L2	36	"
"	10	L1	59	"

[1]From Figure 7:
H2 = High space-averaged luminance × Two-dimensional pattern
L1 = Low space-averaged luminance × One-dimensional pattern
L2 = Low space-averaged luminance × Two-dimensional pattern

Figure 12 depicts contrast sensitivity curves for one- and two-dimensional luminance patterns at low space-averaged luminance using the imputed data set. Visual comparison of Figure 12 and Figure 10 reveals that the inclusion of imputed data produces a minor change at 16 cpd. Otherwise, Figure 12 and Figure 10 are identical.

In a similar manner, Figure 13 depicts space-averaged luminance by stimulus dimension at 8 cpd using the imputed data set. Visual comparison of Figure 13 and Figure 11 reveals no changes resulting from the inclusion of imputed data.

In light of the minor impact of imputed data and the importance of preventing data loss due to missing data, the data set generated by imputing missing values was accepted as a valid data set. This data set was subjected to formal statistical analysis procedures.

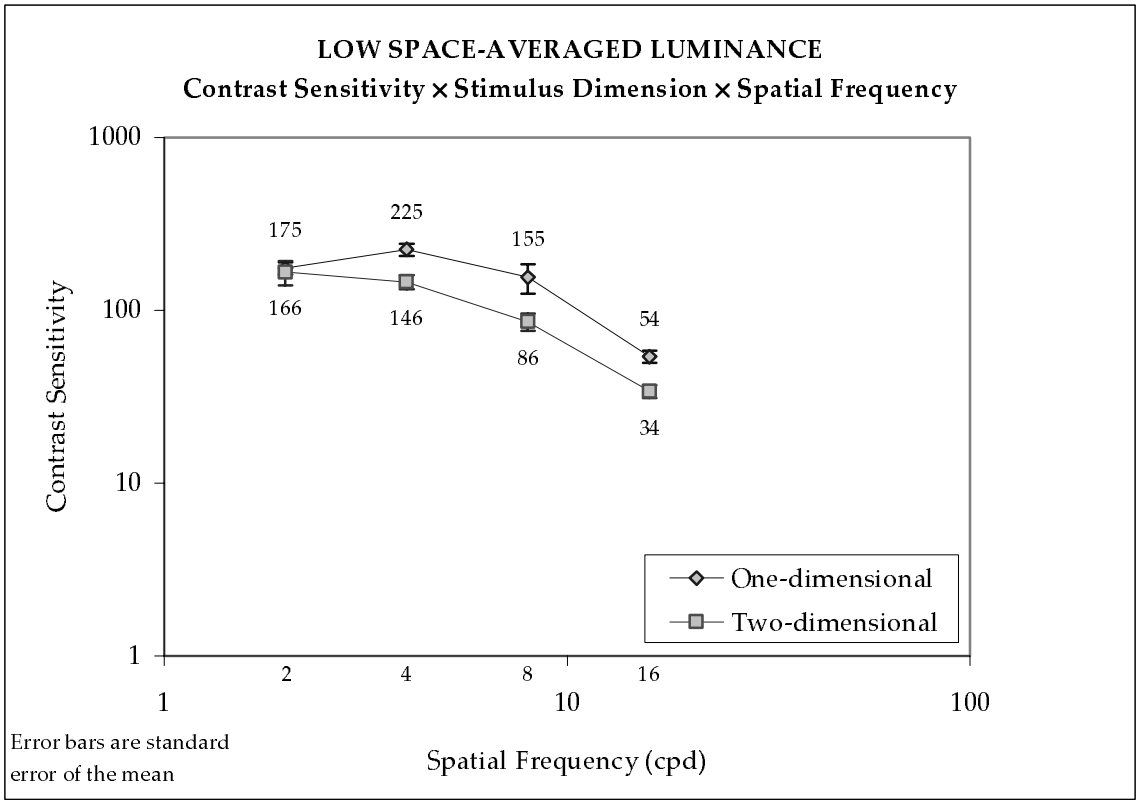

Figure 12. Contrast sensitivity × stimulus dimension × spatial frequency

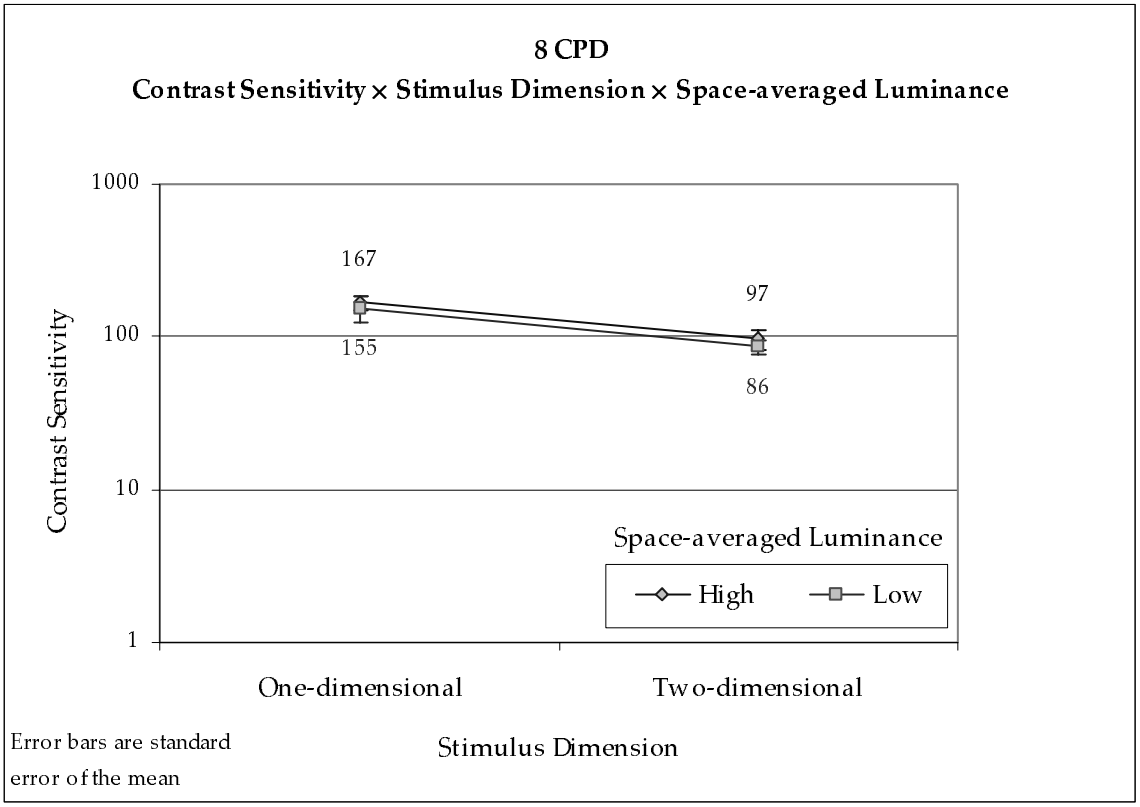

Figure 13. Contrast sensitivity × stimulus dimension × space-averaged luminance

Data Analysis

Statistical tests were conducted in order to evaluate the following research hypotheses:

- Space-averaged Luminance: H_0: $\mu_{high} - \mu_{low} = 0$, H_1: $\mu_{high} - \mu_{low} \neq 0$.
- Stimulus Dimension: H_0: $\mu_{1D} - \mu_{2D} = 0$, H_1: $\mu_{1D} - \mu_{2D} \neq 0$.

Space-averaged Luminance

Data collected at 8 cpd (Table 3 as modified by Table 5) were subjected to an analysis of variance (ANOVA) procedure to test the research hypothesis: H_0: $\mu_{high} - \mu_{low} = 0$ vs. H_1: $\mu_{high} - \mu_{low} \neq 0$.

As reported in Table 6, no main effect of space-averaged luminance was observed. Therefore, the null hypothesis (H_0) is retained. Increasing space-averaged luminance should have increased contrast sensitivity and shifted peak sensitivity to higher spatial frequencies (Norton et al., 2002; Olzak & Thomas, 1986; Thomas, 1975). Consequently, one must conclude that the 25.5 cd/m^2 manipulation of space-averaged luminance was insufficient to produce a measurable difference in observer performance. Further examination of Table 6 reveals a main effect of stimulus dimension ($F(1,7) = 15.863$, $p = .005$) had no significant interaction with space-averaged luminance.

Table 6
ANOVA Summary Table for Contrast Sensitivity at 8 cpd

Source	SS	df	MS	F	η^2	p
S	40261.2	7				
Within S						
Lum	971.649	1	971.649	.392	.053	.551
S × Lum	17339.8	7	2477.114			
Pat	38676.1	1	38676.1	15.863*	.694	.005
S × Pat	17066.5	7	2438.071			
Lum × Pat	2.475	1	2.475	.002	.000	.968
S × Lum × Pat	10127.4	7	1446.771			
Total	124445.1	31				

*significant at $p < .05$
S = Subjects
Lum = Space-averaged Luminance
Pat = Stimulus Dimension

Stimulus Dimension

Data collected under the low space-averaged luminance condition were subjected to an ANOVA procedure to evaluate the research hypothesis: H_0: $\mu_{1D} - \mu_{2D} = 0$, H_1: $\mu_{1D} - \mu_{2D} \neq 0$. Results are reported in Table 7.

Table 7
ANOVA Summary Table for Contrast Sensitivity at 2, 4, 8, and 16 cpd

Source	SS	df	MS	F	η^2	p
S	46014.8	7				
Within S						
Pat	31325.6	1	31325.6	20.076*	.741	.003
S × Pat	10922.4	7	1560.347			
Freq	194309	3	64769.6	32.049*	.821	.000
S × Freq	42440.0	21	2020.953			
Pat × Freq	14360.1	3	4789.698	2.628	.273	.077
S × Pat × Freq	38249.5	21	1821.403			
Total	377621.4	63				

*significant at $p < .05$
S = Subjects
Freq = Spatial Frequency
Pat = Stimulus Dimension

Examination of Table 7 reveals a significant main effect of stimulus dimension ($F(1,7) = 20.076$, $p = .003$). This finding leads to rejection of the null hypothesis (H_0), and one must conclude that stimulus dimension affected observer performance. Specifically, as depicted in Figure 10, contrast sensitivity to one-dimensional luminance patterns was higher than contrast sensitivity to two-dimensional luminance patterns. A main effect of spatial frequency ($F(3,21) = 32.049$, $p = .000$) also was observed. Spatial frequency provided a structural element for the experimental design, functioning primarily as a blocking rather than treatment variable. Therefore, no research hypothesis was evaluated by this result.

DISCUSSION

Preliminary

The following research hypotheses were evaluated using statistical analysis procedures, as described in the previous section. Specific hypotheses were:

- Space-averaged Luminance: H_0: $\mu_{high} - \mu_{low} = 0$, H_1: $\mu_{high} - \mu_{low} \neq 0$.
- Stimulus Dimension: H_0: $\mu_{1D} - \mu_{2D} = 0$, H_1: $\mu_{1D} - \mu_{2D} \neq 0$.

Results revealed that H_0 was retained for space-averaged luminance and rejected for stimulus dimension. The lack of a significant finding for space-averaged luminance most likely arose from the limited range of manipulation of space-averaged luminance to produce a measurable difference in observer performance.

The significant finding that contrast sensitivity to one-dimensional luminance patterns was higher than sensitivity to two-dimensional luminance patterns was not readily understandable within the framework of contemporary spatial vision theory. Contemporary theory, firmly entrenched in data from grating research, models early spatial vision as an array of independent, linear filter mechanisms, each tuned to a narrow range of spatial frequencies and orientations (Graham, 1989; Olzak & Thomas, 1986; Regan, 2000; Wandell, 1995).

Response characteristics of a single filter should predict response characteristics of any other filter sensitive to the same range of spatial frequencies but at different orientations (Campbell & Robson, 1968; Caelli et al., 1983). There, contemporary theory predicts that contrast sensitivity to one-dimensional stimuli should be representative of contrast sensitivity to two-dimensional stimuli.

In fact, the opposite effect might have been anticipated within the framework of probability summation. The notion of probability summation originated from investigation of high threshold theory (Meese & Williams, 2000). Although high threshold theory has been superceded by Signal Detection Theory (Gescheider, 1997; Macmillan & Creelman, 1991; Meese & Williams, 2000), the concept of probability summation remains a highly useful tool for investigating early spatial vision (Manahilov & Simpson, 2001; Meese & Williams, 2000).

Probability summation relates the probability of detecting a stimulus to the number of visual mechanisms (receptive fields) that respond to the spatial frequency and orientation content of the stimulus. As the number of potentially-activated receptive fields increases, the probability of an activation also increases, and thus less contrast modulation would be required for detection (Manahilov & Simpson, 2001; Meese & Williams, 2000).

The symmetric, two-dimensional gratings used in this research simultaneously presented all orientations (0° . . . 360°). Consequently, a large number of spatial vision detectors might have been activated by the two-dimensional pattern, which should have increased the probability of an activation. Thus, based upon a probability summation model, less modulation should have been required for detection of two-dimensional patterns (all orientations) compared to one-dimensional patterns (single orientation).

The fact that observed contrast sensitivity to two-dimensional luminance patterns was not anticipated by a linear filter model or a probability summation model presented an interesting challenge to contemporary spatial vision theory. Alternative explanations were sought.

Fourier Analysis

Kelly and Magnuski (1975) reported an effect of stimulus dimension that was identical to the effect observed in this research. Namely, contrast sensitivity to two-dimensional patterns was lower than sensitivity to one-dimensional patterns. Kelly and Magnuski (1975) reconciled their findings with contemporary theory through application of Fourier analysis. Therefore, Fourier analysis of image data was conducted in an attempt to better understand the significant effect of stimulus dimension.

Kelly and Magnuski (1975) applied Fourier analysis to representative image data (unit amplitude, unit radius). Since they did not apply Fourier analysis to experimental image data, Kelly and Magnuski (1975) implicitly assumed that the spatial vision system was equally sensitive to one- and two-dimensional luminance patterns when these patterns were expressed in the Fourier domain. Kelly and Magnuski (1975) postulated that while modulations in the spatial-domain were different (thus different contrast sensitivities), components of maximum amplitude in the Fourier-domain would be equivalent.

Preparation

Kelly and Magnuski (1975) evaluated a cross section (or slice) of the two-dimensional Fourier transform in order to compare components of maximum amplitude. Whereas Kelly and Magnuski (1975) used representative image data (unit modulation, unit radius), this analysis used image data modulated at experimentally determined threshold values, as summarized in Table 8.

Table 8
Experimentally Determined Modulation Values

Pattern	Spatial Frequency	Modulation*
One-Dimensional	2	0.0057
	4	0.0044
	8	0.0065
	16	0.0185
Two-Dimensional	2	0.0060
	4	0.0068
	8	0.0116
	16	0.0294

*Reciprocal of contrast sensitivity values depicted in Figure 12

For the purposes of optimizing the Fourier analysis, the Gaussian windowing function was removed from image data, and the viewing aperture (in degrees of viewing angle) was increased to eliminate partial frequency cycles (Bores, 2004). In order to eliminate the DC-component and clearly visualize frequency components, Fourier analysis was conducted in number space with real numbers ranging from -1 to +1. Image data were divided by the mean value of the image (DC-component) and then centered on zero by subtracting one (Matlab code: image = image ./ mean2(img) - 1).

In addition to optimizing image data for Fourier analysis, an optimized analysis technique was sought. According to Amidror (1997, 1998), a two-dimensional Discrete Fourier Transform (DFT) generates a Fourier transform with localized DFT artifacts, such as folding over and leakage. This makes interpretation of the central slice of the Fourier transform difficult, as one needs to average the Fourier transform through all angles (0° . . . 360°) to compensate for these artifacts (Amidror, 1997, 1998).

The Fourier Slice Theorem provides a convenient method for evaluating the two-dimensional Fourier transform using a representative one-dimensional Fourier transform (Lun, Hsung, & Shen, 2003). As illustrated in Figure 14, this theorem holds that the one-dimensional Fourier transform of the projection of a two-dimensional image (no rotation) is equivalent to the central slice of the two-dimensional Fourier transform of the image (Lun et al., 2003). The Fourier Slice Theorem generalizes to

projection along any angle of rotation, however only the central slice of the two-dimensional Fourier transform is of interest in this analysis.

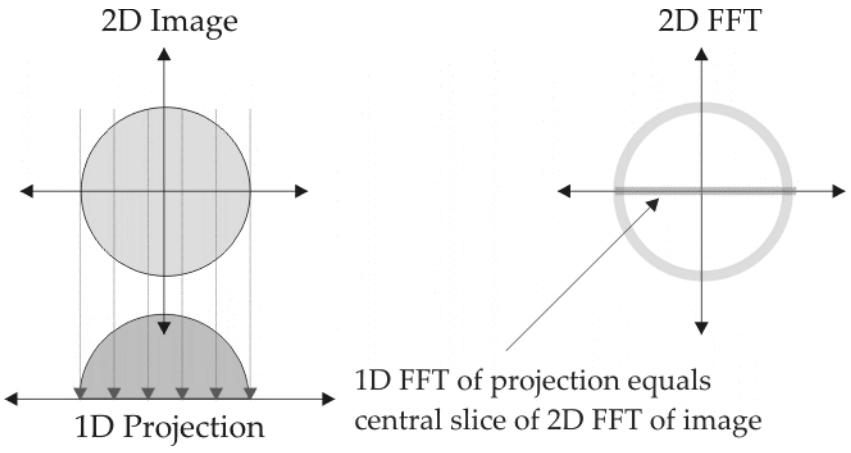

Figure 14. Illustration of Fourier Slice Theorem

Analysis

Analysis was carried out by first generating image data at spatial frequencies and modulations specified in Table 8. Image data then were projected onto an axis with no rotational angle, forming a one-dimensional image vector. Finally, a one-dimensional DFT was applied to the projected image vector. Equation 8 provides a formal mathematical definition for the one-dimensional DFT (Weisstein, 2004a).

$$F_n \equiv \sum_{k=0}^{N-1} f_k e^{-2\pi i n k/N}$$

Equation 8

Where,

- F_n is the complex-valued Fourier transform vector;
- f_k is the real-number image vector ranging from -1 to +1; and
- N is the length of the image vector.

The frequency spectrum was obtained by taking the complex modulus of Fourier transform vector, as specified in Equation 9 (Weisstein, 2004b).

$$|F_n| = |x + iy| = \sqrt{x^2 + y^2}$$

Equation 9

Where,

- x is the real part of F_n, and
- iy is the imaginary part of F_n.

The negative frequency portion of the transform vector was removed and the retained portion scaled by a factor of two to compensate (shown as Figure 15, Figure 16, Figure 17, and Figure 18). Table 9 summarizes these results.

Table 9
Maximum Component Magnitudes

Pattern	Spatial Frequency	Maximum Component Magnitude*
One-dimensional	2	0.00569
	4	0.00439
	8	0.00643
	16	0.01774
Two-dimensional	2	0.00064
	4	0.00048
	8	0.00055
	16	0.00095

*Evaluated for the central slice of the 2D DFT through application of Fourier Slice Theorem

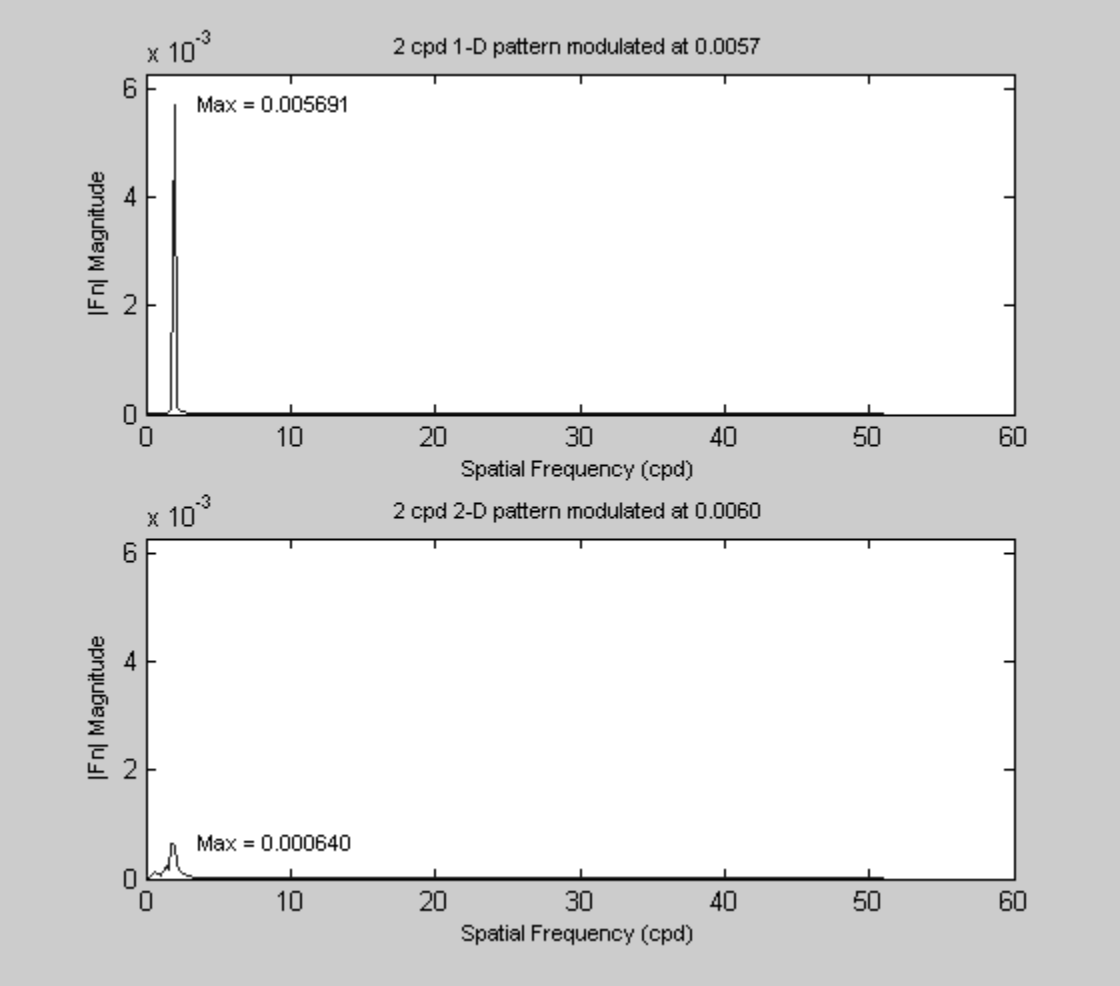

Figure 15. Maximum component magnitudes at 2 cpd

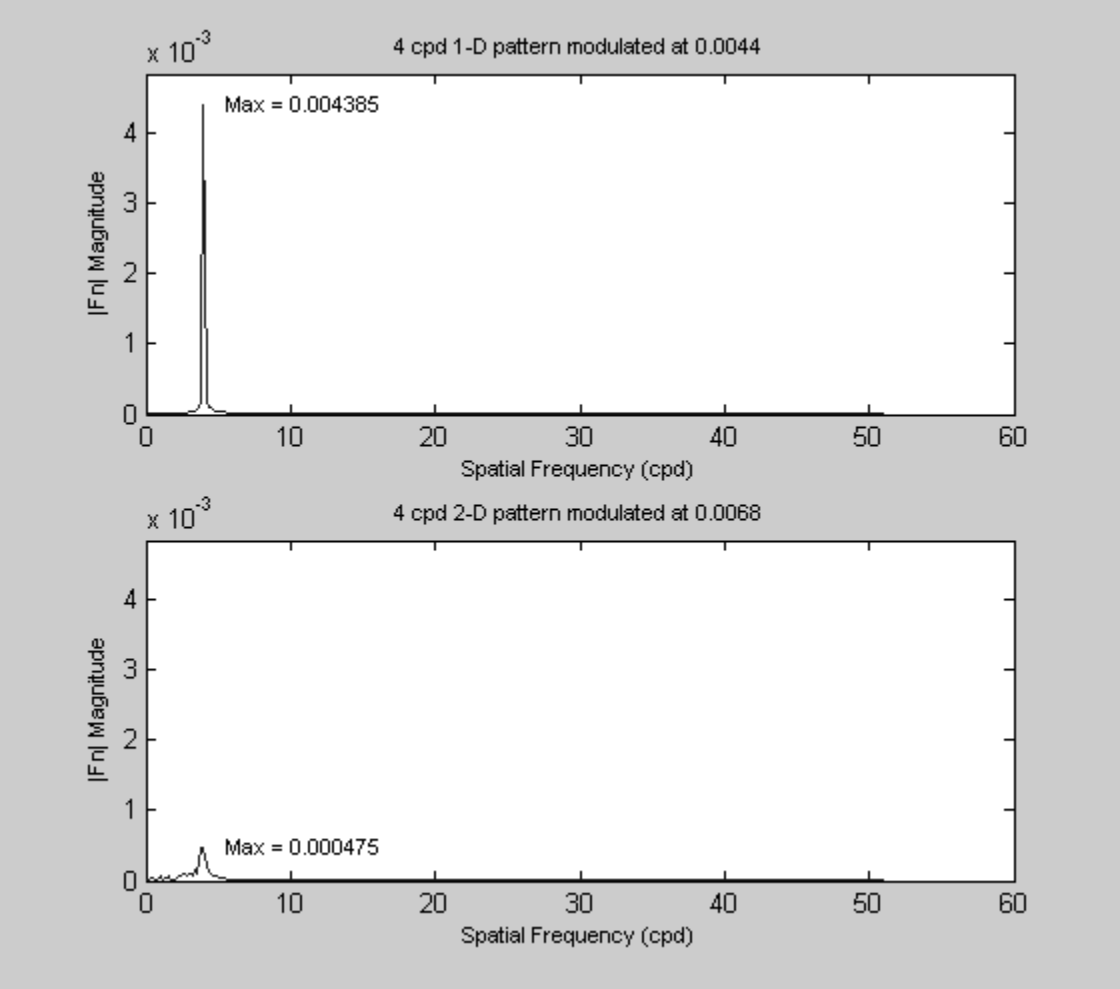

Figure 16. Maximum component magnitudes at 4 cpd

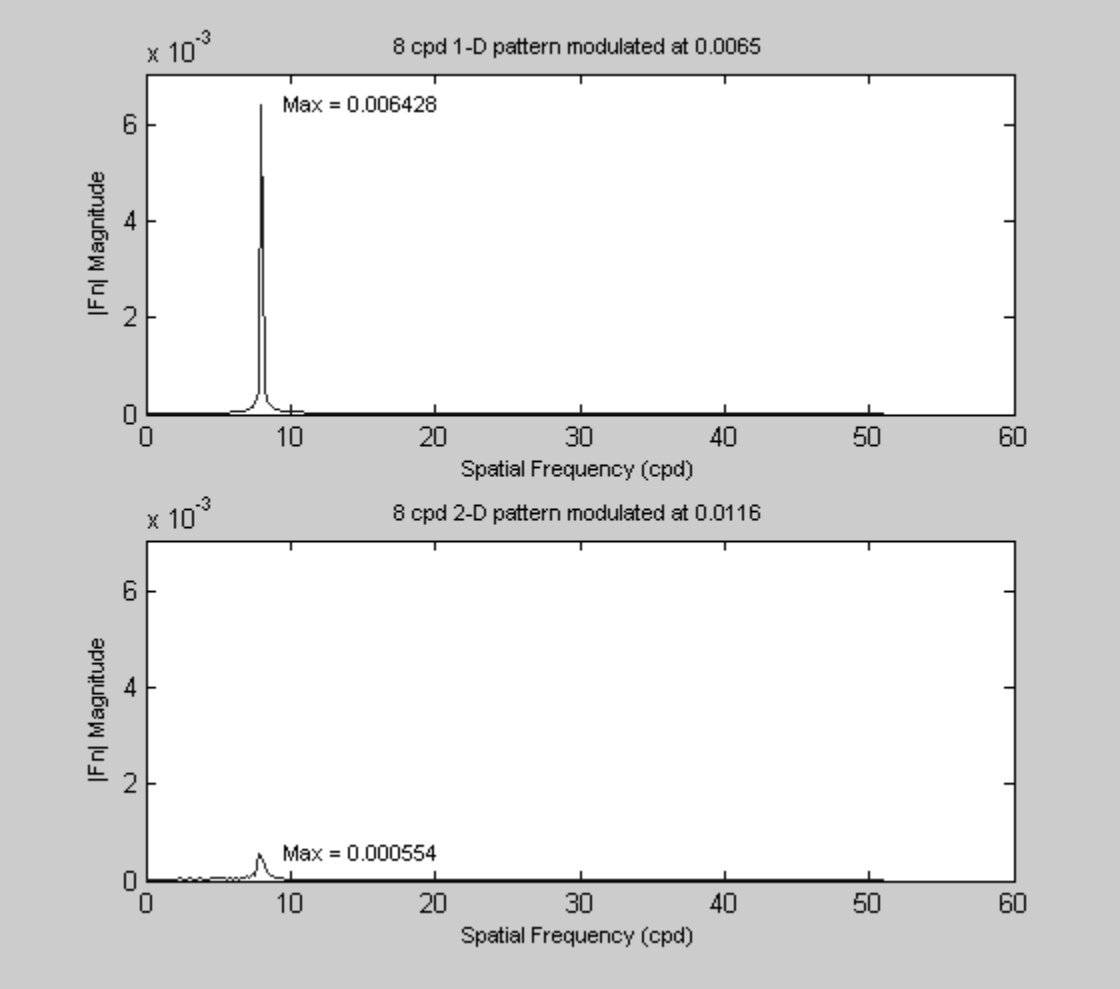

Figure 17. Maximum component magnitudes at 8 cpd

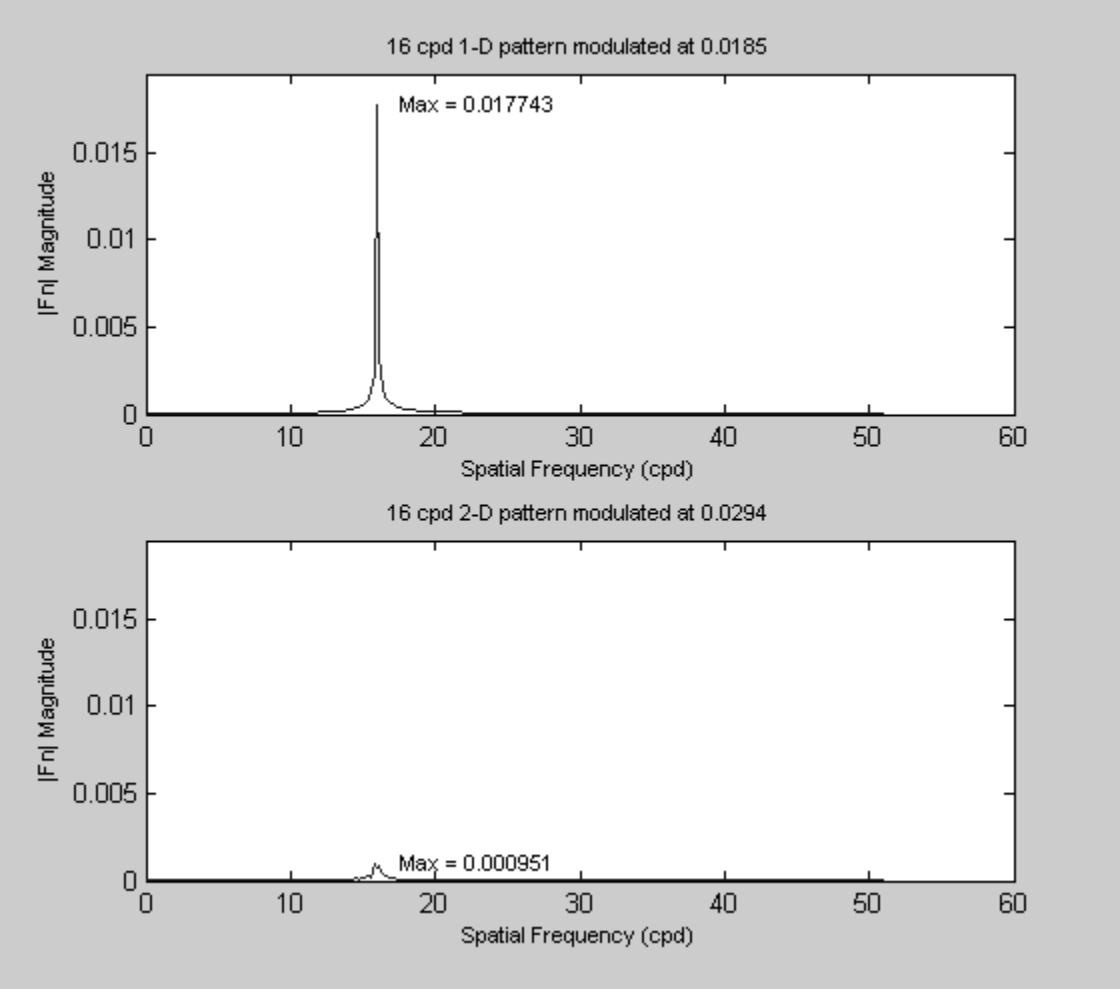

Figure 18. Maximum component magnitudes at 16 cpd

Fourier Results

Examination of Table 9 reveals that maximum component magnitudes of one- and two-dimensional patterns were not equivalent in the Fourier-domain. Magnitudes for two-dimensional patterns were lower than magnitudes for one-dimensional patterns. This result was anticipated given that the Fourier transform of a one-dimensional pattern concentrates available energy into a point at the spatial frequency coordinate, whereas the Fourier transform of a two-dimensional pattern spreads energy over a ring with radius proportional to the spatial frequency (Kelly & Magnuski, 1975).

Interpretation

Kelly and Magnuski (1975) postulated that while contrast sensitivity to one- and two-dimensional luminance patterns might be different in the spatial-domain, components of maximum amplitude in the Fourier-domain would be equivalent. In their analysis, Kelly and Magnuski (1975) applied Fourier analysis to image data with unit modulation, which represented experimental conditions. The Fourier analysis reported in this research was applied to image data that were modulated at experimentally derived values that reproduced experimental conditions.

As reported in Table 9, maximum component magnitudes of one- and two-dimensional luminance patterns were not equivalent in the Fourier-domain. Consequently, one must reject the notion put forth by Kelly and Magnuski (1975) that human spatial vision could be less sensitive to two-dimensional luminance patterns in the spatial-domain but equally sensitive in the Fourier-domain when compared to one-dimensional luminance patterns. Alternative explanations for experimentally observed contrast sensitivity differences between one- and two-dimensional luminance patterns were sought.

On/Off Receptive Fields

Norton et al. (2002) presented data describing on/off receptive field mechanisms. Receptive fields mechanisms conformed to response characteristics of a linear filter model, as suggested by contemporary spatial vision theory. Namely, an array of linear filters, each tuned to a narrow range of spatial frequencies and orientations (Graham, 1989; Olzak & Thomas, 1986; Regan, 2000; Wandell, 1995).

In addition to linear filter response characteristics, receptive fields also exhibited either on-center or off-center response characteristics, as shown in Figure 19. When the central portion of a receptive field was activated, its output was either excitatory (on-center) or inhibitory (off-center), and the surround portion produced an opposite response (i.e., on-center → off-surround and off-center → on-surround) (Norton et al., 2002). The rate of at which action potentials were generated varied with the degree of similarity between the response characteristics of the receptive field and the frequency and orientation of the input stimulus (Norton et al., 2002).

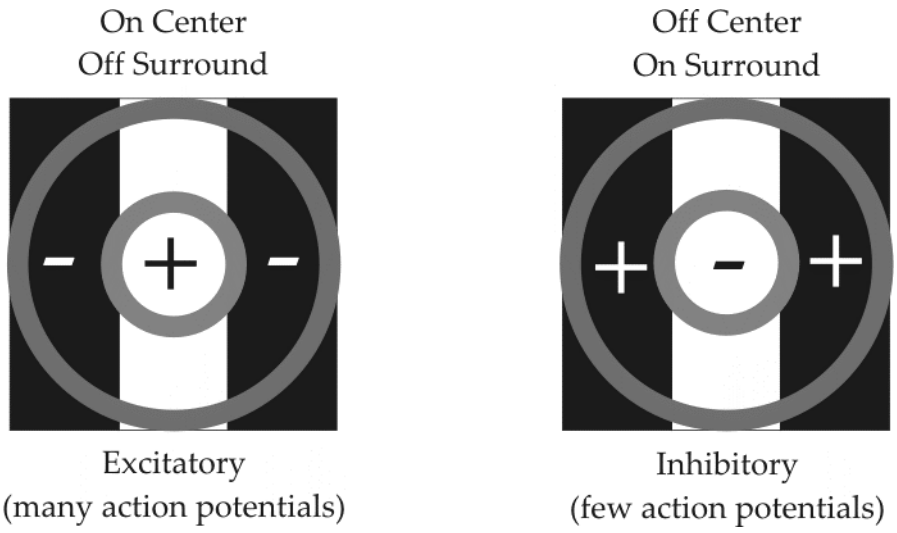

Figure 19. On-center vs. off-center receptive fields

The one-dimensional patterns used in this research would have activated receptive field mechanisms tuned to a specific spatial frequency and orientation. On the other hand, the two-dimensional, symmetric patterns used in this research would have activated receptive field mechanisms tuned to a specific spatial frequency but at all orientations. The additional orientation information contained in two-dimensional luminance patterns might have generated a greater number of action potentials (either excitatory or inhibitory) relative to one-dimensional luminance patterns. Therefore, contrast sensitivity to two-dimensional patterns might have been reduced because of increased neural activity due to activation of a greater number of receptive field mechanisms.

The receptive field model provided a good explanation of results reported in this research. However, results reported by Kelly and Magnuski (1975) were more difficult to explain in terms of this model. In their research, Kelly and Magnuski (1975) found that, at low spatial frequencies (less than 1 cpd), contrast sensitivity to two-dimensional patterns was higher than sensitivity to one-dimensional patterns. Excitatory and inhibitory neural activity associated with receptive field mechanisms does not provide a sufficient explanation.

Watershed Behavior

Campbell et al. (1981) proposed a watershed model of the spatial vision system to account for low frequency roll-off of contrast sensitivity to sinusoidal gratings. In this model, the spatial vision system responds to luminance gradients rather than spatial frequency content at low spatial frequencies (approximately 1 cpd and lower). This behavior was peculiar to one-dimensional sinusoidal patterns and was not observed

with trapezoidal, square, or triangular gratings (Campbell et al.). If low frequency roll-off is restricted to the one-dimensional class of sinusoidal patterns, then watershed behavior would account for higher contrast sensitivity to two-dimensional vs. one-dimensional luminance patterns at low spatial frequencies, as reported by Kelly and Magnuski (1975).

Ecological Behavior

The notion of watershed behavior perhaps hints at a deeper, ecological behavior of the visual system. Essock, DeFord, Hansen, and Sinai (2003) investigated the oblique effect of spatial vision using gratings embedded in broadband noise representing a naturalistic environment. Quite surprisingly, Essock et al. found that oblique gratings were more detectable than either horizontally or vertically oriented gratings. This effect was the opposite of the usual oblique effect in which horizontal or vertical gratings would be more detectable than oblique gratings (e.g., De Valois, Yund, & Hepler, 1982; Caelli et al., 1983).

Essock et al. (2003) suggested that traditional grating research frequently failed to include ecological context in the experimental design, thereby reducing the generalizability of research findings. This notion was not without merit, given that a real-world visual scene is two-dimensional in nature with a myriad of spatial frequencies and orientations. However, one must be cautious in adopting naturalistic frameworks that depart from rigorous experimental methods (Kvavilashvili & Ellis, 1996).

From the standpoint of Kvavilashvili and Ellis (1996), the two-dimensional stimulus patterns used in this research represented an outstanding tool for investigating spatial vision function. The two-dimensional patterns provided a naturalistic stimulus that better represented real-world, two-dimensional spatial vision compared to one-dimensional patterns. More importantly, the two-dimensional pattern used in this research provided a direct, two-dimensional analog to one-dimensional patterns, thereby inheriting the generalizable utility of one-dimensional patterns (Olacsi, 2001).

Impact

This research has shown that contrast sensitivity to two-dimensional luminance patterns is lower than sensitivity to one-dimensional luminance patterns. Table 10 summarizes the difference between sensitivity to two-dimensional vs. one-dimensional luminance patterns.

Table 10
Percent Difference Between 2D and 1D Detection Thresholds

Spatial Frequency (cpd)	Threshold (% modulation, 1D)*	Threshold (% modulation, 2D)*	2D - 1D Threshold Difference (%)
2	0.0057	0.0060	5
4	0.0044	0.0068	35
8	0.0065	0.0116	45
16	0.0185	0.0294	37

*Reciprocal of contrast sensitivity values depicted in Figure 12

Examination of Table 10 reveals that detection thresholds for two-dimensional luminance patterns were approximately 5% to 45% lower than thresholds for one-dimensional luminance patterns. This results suggests that the model developed by Olasci (2001) might over predict observer performance. The general shape of the contrast sensitivity curves (see Figure 12) were similar. Therefore, there is no reason to doubt the conclusions drawn by Olacsi (2001); however, the model might benefit from inclusion of the two-dimensional spatial vision data reported in this research.

From an engineering standpoint, the results reported in this research might suggest that operator performance models based upon one-dimensional spatial vision data might over predict operator performance. That is to say that systems design on the basis of one-dimensional spatial vision models might be improved by recognizing the diminished capability of spatial vision in real-world, non-laboratory settings (i.e., real world visual scenes are two-dimensional in spatial extent with spatial frequency information available at all orientations).

From a theoretical standpoint, the results reported in this research might suggest further exploration of eye-brain mechanisms responsible for spatial vision. Certainly the model of independent linear filter mechanisms, sensitive to a limited range of spatial frequency and orientation is inadequate to explain reported results. The question at

hand is whether early or late processing might be responsible for reducing sensitivity to two-dimensional luminance patterns. Ecological spatial vision research (e.g., Essock et al., 2003) suggests that late processes, deeper in the eye-brain system might be responsible for mediating spatial vision of real-world scenes. Additional spatial vision investigation with two-dimensional luminance patterns is warranted.

CONCLUSIONS

This research investigated contrast sensitivity to one- and two-dimensional luminance patterns in an effort to fill theoretical gaps produced by 40 years of spatial vision modeling based upon grating research with one-dimensional luminance patterns. The following research hypotheses were tested:

- Space-averaged Luminance: H_0: $\mu_{high} - \mu_{low} = 0$, H_1: $\mu_{high} - \mu_{low} \neq 0$.
- Stimulus Dimension: H_0: $\mu_{1D} - \mu_{2D} = 0$, H_1: $\mu_{1D} - \mu_{2D} \neq 0$.

Statistical tests revealed that H_0 was retained for space-averaged luminance and rejected for stimulus dimension. The result for space-averaged luminance likely arose from the limited range of manipulation of space-averaged. The range was too small to produce a measurable difference in observer performance.

The finding that contrast sensitivity to two-dimensional patterns was lower than sensitivity to one-dimensional patterns was explained in terms of an on-center, off-center receptive field model coupled with watershed behavior at spatial frequencies below 1 cpd. The additional orientation information in two-dimensional patterns was thought to produce a greater number of excitatory and inhibitory action potentials, thereby decreasing contrast sensitivity relative to one-dimensional patterns. Watershed behavior accounted for higher sensitivity to two-dimensional vs. one-dimensional patterns at spatial frequencies below 1 cpd.

This research filled a crucial void left in the work of Olacsi (2001). Results reported in this document suggest that the model developed by Olacsi (2001) might over predict operator performance from between 5% to 45%. The general gist of Olacsi (2001) was supported by this research in that spatial vision response to two-dimensional luminance patterns was consistent with spatial vision response to one-dimensional luminance patterns. Specifically, both contrast sensitivity curves (see Figure 12) demonstrated a bandpass shape with roll-off in contrast sensitivity at high spatial frequencies.

The use of two-dimensional patterns was central to producing results reported in this research. One-dimensional patterns would not have provided similar results. Spatial vision models based upon one-dimensional patterns might not be adequate, in that these models might not include ecological context. Consequently, models based upon one-dimensional patterns might be too sensitive or not sensitive enough, depending upon the ecological context.

Future research might explore the relationship between probability summation and orientation information in an experiment using partial two-dimensional patterns, such as quarter- or half-circle patterns. Partial two-dimensional patterns would maintain a consistent spatial frequency while manipulating different levels of orientation information. In a similar manner, orientation bandwidths and sensitivity might be re-evaluated within a two-dimensional framework to understand whether traditional visual phenomenon such as the oblique effect retain validity in a two-dimensional construct.

REFERENCES

Amidror, I. (1997). Fourier spectrum of radially periodic images. *Journal of the Optical Society of America (A), 14,* 816–826.

Amidror, I. (1998). The Fourier-spectrum of circular sine and cosine gratings with arbitrary radial phases. *Optics Communications, 149,* 127–134.

Beaton, R. J. (1983). *Quality metrics of digitally derived imagery and their relation to intepreter perfomance: VII. Evaluation of quality metrics (Technical Report, HFL-83-5).* Blacksburg, VA: Virginia Polytechnic Institute and State University.

Bracewell, R. N. (1986). *The fourier transform and its applications* (Rev. ed.). New York: McGraw-Hill Book Company.

Bores, J. (2004). *Advanced DSP*. Retrieved March 28, 2004 from Bores Signal Processing Web site: http://www.bores.com/courses/advanced/index.htm.

Caelli, T., Brettel, H., Rentschler, I., & Hilz, R. (1983). Discrimination thresholds in the two-dimensional spatial frequency domain. *Vision Research, 23,* 129–133.

Campbell, F. W., Johnstone, J. R., & Ross, J. (1981). An explanation for the visibility of low frequency gratings. *Vision Research, 21,* 723–730.

Campbell, F. W., & Robson, J. G. (1968). Application of Fourier analysis to the visibility of gratings. *Journal of Physiology, 197,* 551–566.

Derrington, A. M., & Henning, G. B. (1989). Some observations on the masking effects of two-dimensional stimuli. *Vision Research, 29,* 241–246.

De Valois, R. L., Yund, E. W., & Hepler, N. (1982). The orientation and direction selectivity of cells in macaque visual cortex. *Vision Research, 22,* 531–544.

Essock, E. A., DeFord, J. K., Hansen, B. C., and Sinai, M. J. (2003). Oblique stimuli are seen best (not worst!) in naturalistic broad-band stimuli: a horizontal effect. *Vision Research, 43,* 1329–1335.

Ferwerda, J. A., Shirley, P., Pattanaik, S. N., & Greenberg, D. P. (1997). A model of visual masking for computer graphics. *Proceedings of the 24th annual conference on Computer graphics and interactive techniques,* 143–152.

Gescheider, G. A. (1997). *Psychophysics: The fundamentals* (3rd ed.). Mahwah, NJ: Lawrence Erlbaum Associates, Inc.

Graham, N. (1989). *Visual pattern analyzers.* New York: Oxford University Press, Inc.

Greenlee, M. W., & Magnussen, S. (1987). Higher-harmonic adaptation and the detection of squarewave gratings. *Vision Research, 27,* 249–255.

Guilford, J. P. (1954). *Psychometric methods.* New York: McGraw–Hill Book Company.

Hoekstra, J., Van Der Goot, D. P. J., Van Den Brink, G., & Bilsen, F. A. (1974). The influence of the number of cycles upon the visual threshold for spatial sine wave patterns. *Vision Research, 14,* 365–368.

Howell, D. C. (1987). *Statistical methods for psychology* (2nd ed.). Boston: PWS-Kent Publishing Company.

Kelly, D. H., & Magnuski, H. S. (1975). Pattern detection and the two-dimensional Fourier transform: Circular targets. *Vision Research, 15,* 911–915.

Klein, S. A. (2001). Measuring, estimating, and understanding the psychometric function: A commentary. *Perception & Psychophysics, 63,* 1421–1455.

Kvavilashvili, L. & Ellis, J. (1996). Let's forget the everyday/laboratory controversy. *Behavioral and Brain Sciences, 19,* 199-200.

Lun, D. P. K., Hsung, T. C., & Shen, T. W. (2003). Orthogonal discrete periodic Radon transform: II. Applications. *Signal Processing, 83,* 957–971

Macmillan, N. A., & Creelman, C. D. (1991). *Detection theory: A user's guide*. New York: Cambridge University Press.

Manahilov, V., & Simpson, W. A. (2001). Energy model for contrast detection: Spatial-frequency and orientation selectivity in grating summation. *Vision Research, 41,* 1547–1560.

Meese, T. S., & Williams, C. B. (2000). Probability summation for multiple patches of luminance modulation. *Vision Research, 40,* 2101–2113.

Norton, T. T., Lakshminarayanan, V., & Bassi, C. J. (2002). Spatial Vision. In T. T. Norton, D. A. Corliss, & J. E. Bailey (Eds.), *The psychophysical measurement of visual function*. Boston: Butterworth-Heinemann.

Neurometrics Institute. (2003). WinVis W4M [Computer software and manual]. Retrieved September 5, 2003, from http://www.neurometrics.com/winvis/index.jsp

Olacsi, G. S. (2001). *Examining visual masking effects on target acquisition using two-dimensional Fourier analysis techniques*. Unpublished doctoral dissertation, Virginia Polytechnic Institute and State University, Blacksburg.

Olzak, L. A., & Thomas, J. P. (1986). Seeing spatial patterns. In K. R. Boff, L. Kaufman, & J. P. Thomas (Eds.), *Handbook of perception and human performance: Vol. 1. Sensory processes and perception*. New York: John Wiley and Sons.

Regan, D. (2000). *Human perception of objects: Early visual processing of spatial form defined by luminance, color, texture, motion, and binocular disparity*. Sunderland, MA: Sinauer Associates, Inc.

Robson, J. G. (1975). Receptive fields: Neural representation of the spatial and intensive attributes of the visual image. In E. C. Carterette & M. P. Friedman (Eds.), *Handbook of perception: Vol. 5. Seeing*. New York: Academic Press, Inc.

Schafer, J. L. (1999). NORM: Multiple imputation of incomplete multivariate data under a normal model (Version 2) [Computer software]. Retrieved March 20, 2004, from http://www.stat.psu.edu/~jls/misoftwa.html.

Strasburger, H. (2001). Invariance of the psychometric function for character recognition across the visual field. *Perception & Psychophysics, 63,* 1356–1376.

Thomas, J. P. (1975). Spatial resolution and spatial interaction. In E. C. Carterette & M. P. Friedman (Eds.), *Handbook of perception: Vol. 5. Seeing*. New York: Academic Press, Inc.

VisTech Consultants, Inc. (1990). *Vision Contrast Test System (VCTS 6500)*. Dayton, OH: Author.

Wandell, B. A. (1995). *Foundations of vision*. Sunderland, MA: Sinauer Associates, Inc.

Watanabe, A., Mori, T., Nagata, S., & Hiwatashi, K. (1968). Spatial sine-wave responses of the human visual system. *Vision Research, 8,* 1245–1263.

Weisstein, E. W. (2004a). *Discrete Fourier transform*. Retrieved March 22, 2004, from MathWorld – A Wolfram Web Resource site http://mathworld.wolfram.com/DiscreteFourierTransform.html

Weisstein, E. W. (2004b). *Complex modulus*. Retrieved March 22, 2004, from MathWorld – A Wolfram Web Resource site http://mathworld.wolfram.com/ComplexModulus.html

Wichmann, F. A., & Hill, N. J. (2001a). The psychometric function: I. Fitting, sampling, and goodness of fit. *Perception & Psychophysics, 63,* 1293–1313.

Wichmann, F. A., & Hill, N. J. (2001b). The psychometric function: II. Bootstrap-based confidence intervals and sampling. *Perception & Psychophysics, 63,* 1314–1329.

Wilkinson, F., Wilson, H. R., & Habak, C. (1998). Detection and recognition of radial frequency patterns. *Vision Research, 38,* 3555–3568.